U.PORTO
FEUP FACULDADE DE ENGENHARIA
UNIVERSIDADE DO PORTO

INSTITUTO DE INVESTIGAÇÃO
E INOVAÇÃO EM SAÚDE
UNIVERSIDADE DO PORTO

M 2021

DEVELOPMENT OF A HYDROGEL-BASED DELIVERY MATRIX TO REGULATE BONE CELL DIFFERENTIATION WITH APPROPRIATED RHEOLOGICAL PROPERTIES TO BE LOADED INTO A 3D POROUS SCAFFOLD

ANA CATARINA LEAL COSTA

DISSERTATION FOR THE MASTER'S DEGREE IN METALLURGICAL AND MATERIALS ENGINEERING AT THE FACULTY OF ENGINEERING OF UNIVERISTY OF PORTO

SUPERVISOR
Professor Doctor Fernando Jorge Mendes Monteiro

CO-SUPERVISOR
Doctor Christiane Laranjo Salgado

CANDIDATE	Ana Catarina Leal Costa	*Code*	201603959
TITLE	Development of a hydrogel-based delivery matrix to regulate bone cell differentiation with appropriated rheological properties to be loaded into a 3D porous scaffold		
JURI	*President*	Maria Ascensão Ferreira Silva Lopes	DEMM-FEUP
	Examiner	Susana Maria Ribeiro e Sousa Mendes de Freitas	DEQ-ISEP/i3s
	Supervisor	Fernando Jorge Mendes Monteiro	DEMM-FEUP
DATE	*19th July 2021*		
TIME	*9h00*		

The important thing is not to stop questioning. Curiosity has its own reason for existing. One cannot help but be in awe when he contemplates the mysteries of eternity, of life, of the marvellous structure of reality. It is enough if one tries merely to comprehend a little of this mystery every day. Never lose a holy curiosity.

Albert Einstein

Abstract

Maxillofacial bone defects are typically associated with trauma, osteonecrosis, tumor removal, or congenital disorders. Patients with these disorders experiment with amputation of large portions of hard tissue, significantly decreasing the quality of their lives and causing very limitative disabilities. Bone tissue engineering plays an important role to develop solutions for these clinical problems. Collagen/nanohydroxyapatite (Coll/nanoHA) scaffolds and Fibrin (Fb) Hydrogels are widely used in the tissue engineering field as biomaterials. The mechanical and biological performance of fibrin hydrogel is directly dependent on its composition (Fibrinogen and Thrombin (Tb) concentrations).

The main goal of this dissertation work was to offer a three-dimensional (3D) Coll/nanoHA scaffold containing fibrin hydrogel to improve the mechanical properties of the graft and enhance its regenerative properties. Fibrinogen and/or thrombin concentrations were evaluated into the hydrogel construct by standard rheological/mechanical testing. To boost bone regeneration, the fibrin-based hydrogel was improved via Osteopontin (OPN) immobilization to fibrin. The mechanical properties of the composite (Coll/nanoHA + Fb Hydrogel with and/or without OPN) were characterized by Dynamic Mechanical Analysis assay (Storage Modulus, Loss Modulus, Loss Factor). Subsequently, the Fb hydrogel and Fb Hydrogel + OPN viscoelasticity was evaluated by rheometer analysis (Storage and loss modulus) under shear stress compression. As a biodegradable composite, the cytotoxicity of the materials degradation products was evaluated by indirect *in vitro* assay with a standard cell line (MG63). Cell viability, ECM components, and cell differentiation capacity of the composite were analysed.

Mechanical characterization has shown an improvement in the strength of the scaffold with the incorporation of the Fb Hydrogel. The thrombin content promoted an enhancement at the mechanical properties of the Fb hydrogel when compared to the Fb content. To an optimal concentration of 6.3 mg/mL of fibrinogen and 2 NHI (U/mL) of thrombin (Coll/nanoHA_Fb 1:2 HTb composite), the mechanical strength of the Coll/nanoHA scaffold was improved, maintaining its elasticity. Biologically, the composite Coll/nanoHA_Fb 1:2 HTb with and without OPN protein exhibited high cell viability, increasing the new bone-cell formation with time culture (1,3 and 6 days). ALP activity of the composite showed at day 6 of culture higher osteoblastic phenotype expression. Histocytochemical staining showed high type I collagen and mineral calcium phosphate deposition with the increase of time in culture. OPN protein incorporation provided high cell differentiation and proliferation without affecting the mechanical properties of the composite. Hence, Coll/nanoHA/Fb scaffold evidenced a potential solution to improve successful bone tissue regeneration in patients with maxillofacial bone defects.

Key-Words: Biomaterials; Hydrogel; Fibrin; Collagen; Nanohydroxyapatite; Rheological Properties

Resumo

Os defeitos ósseos maxilofaciais estão normalmente associados a traumas, osteonecrose, remoção de tumores, ou desordens congénitas. Associado a este problema os doentes são sujeitos a amputações de grandes porções de massa óssea, o que diminui significativamente a sua qualidade de vida, causando incapacidades muito limitativas. A engenharia de tecidos ósseos desempenha um papel fundamental no desenvolvimento de soluções para estes problemas clínicos. Os scaffolds de colagénio/nanohidroxiapatite (Coll/nanoHA) e hidrogéis de Fibrina (Fb) são amplamente utilizados no campo da engenharia de tecidos como biomateriais. O desempenho mecânico e biológico do hidrogel à base de fibrina está diretamente dependente da sua composição (concentração de Fibrinogénio e Trombina (Tb)).

O principal objetivo desta dissertação foi desenvolver um scaffold tridimensional (3D) de Coll/nanoHA contendo hidrogel de fibrina como forma de melhorar as propriedades mecânicas do scafolld, bem como as suas propriedades regenerativas. As concentrações de fibrinogénio e/ou trombina foram avaliadas na construção do hidrogel através de testes reológicos/mecânicos padrão. Para impulsionar a regeneração óssea, o hidrogel à base de fibrina foi melhorado através da imobilização de Osteopontina (OPN) à fibrina. As propriedades mecânicas do composto (Coll/nanoHA + Hidrogel de Fb com e/ou sem OPN) foram caraterizadas pelo ensaio de Análise Mecânica Dinâmica (Módulo de Armazenamento, Módulo de Perda, Fator de Perda). Subsequentemente, a viscoelasticidade do hidrogel de Fb e hidrogel de Fb + OPN foi avaliada por análise reológica (Módulo de Armazenamento e Módulo de Perda) sob uma de tensão de corte. Como composto biodegradável, a citotoxicidade dos produtos de degradação do compósito foi avaliada por ensaio indireto *in vitro* com uma linha celular padrão (MG63). Foi analisada a viabilidade celular, composição matriz extracelular (ECM), e a capacidade de induzir a diferenciação celular pelo compósito.

A caracterização mecânica mostrou uma melhoria na resistência do scaffold com a incorporação do Hidrogel de Fb. O teor de trombina promoveu uma melhoria mais significativa nas propriedades mecânicas do Fb hidrogel, quando comparado com o teor de Fb. Para uma concentração ótima de 6,3 mg/mL de fibrinogénio e 2 NHI (U/mL) de trombina (compósito Coll/nanoHA_Fb 1:2 HTb), a resistência mecânica do scaffold Coll/nanoHA foi melhorada, mantendo a sua elasticidade. Biologicamente, o compósito Coll/nanoHA_Fb 1:2 HTb com e sem OPN, demonstrou uma elevada viabilidade celular, aumentando a diferenciação celular para células ósseas com o tempo de cultura (1,3 e 6 dias). A atividade do ALP das células mostrou para o dia 6 de cultura celular uma elevada expressão fenotípica osteoblástica. A coloração histoquímica evidenciou uma elevada deposição de colagénio do tipo 1 e de minerais a base de fosfato de cálcio com o aumento do tempo de cultura. A incorporação da proteína OPN proporcionou elevada proliferação e diferenciação celular no compósito sem afetar as suas propriedades mecânicas. Assim, Coll/nanoHA/Fb scaffold mostrou ser uma potencial solução para promover a regeneração do tecido ósseo bem sucedida em pacientes com defeitos ósseos maxilofaciais.

Palavras-chave: Biomateriais; Hidrogel; Fibrina; Colagénio; Nanohidroxiapatite; Propriedades Reológicas

Acknowledgements

This work completes five years of a short, but marvellous journey in my academic and personal life. With all my love, I would like to let here my deepest gratitude to all the people that support me and help me to reach this day.

Firstly, I would like to thank my supervisor Professor Doctor Fernando Jorge Monteiro, which provided me the marvellous opportunity of taking part in this project. It was a true honour taking you as my supervisor. For me, the Professor represents the highest role model of a professional that one day I would like to achieve.

Secondly, I would like to express my deepest gratitude to my co-supervisor Doctor Christiane Laranjo Salgado, which since the first day was always supportive of me. She thought me, helped me, and inspired me with this project. Thank you, Doctor Christiane, for being always available for absolutely everything that I needed. It was a true pleasure to know you and learn from you. You are a noble reference for me.

To Ricardo Vidal (i3s) for all the technical support that I needed for this project and all biocomposites group members for receiving me so well in their group.

To all the teachers in the Department of Metallurgical and Materials Engineering at FEUP, for enriching me with academic knowledge and personal growth.

To my beautiful and incredible friends, I would like to thank you for always supporting me, helping me, and making these five years unforgettable. Thank you, Helder, Inês, Liliane, and Susana, is more than an honour to have you in my life.

To my entire family, and especially to my cousin, and incredible friend, Filipa, for always supporting me in every stage in my life.

To all my work colleagues (Mc Donald's) for making the last two years of my life smoother and funnier. I would like to especially most profound thank you to my work colleague Márcia Rocha for being incredible and helping me and supporting me with everything I needed for this work.

And last – but most certainly, not the least, the most important people in my life. I would like to thank my mother, father, and brother, for being the biggest support of my life, and never, ever let me be less than happy. You are all a reference for me. I am the most profound lucky person for having every single of you every day by my side.

Contents

Abstract ____ *iv*

Resumo ____ *v*

Acknowledgements ____ *vi*

LIST OF FIGURES ____ *x*

LIST OF TABLES ____ *xiv*

LIST OF ABBREVIATIONS ____ *xv*

Chapter 1 ____ *1*

Objectives and Document Structure ____ *1*

1.1 Objectives of the work ____ *1*

1.2 Document structure ____ *1*

Chapter 2 ____ *2*

Literature Review ____ *2*

2.1 Introduction ____ *2*

2.2 Bone ____ *3*

2.2.1 Function ____ **3**

2.2.2 Structure ____ **3**

2.2.3 Constitution ____ **4**

2.2.3.1 Collagen ____ 5

2.2.3.2 Nanohydroxyapatite ____ 6

2.2.4 Bone Repair Process ____ **6**

2.2.4.1 Osteopontin in Bone Repair ____ 7

2.2 Bone Tissue Engineering ____ *8*

2.2.1 Scaffolds ____ **8**

2.2.2 Biomaterials ____ **9**

2.2.1.1 Bioceramics ____ 10

2.2.1.2 Polymers ____ 10

2.2.3 Polymer/Bioceramic Scaffolds ____ **11**

2.2.4 Scaffolds Production Techniques ____ **11**

2.3.4.1 Cryogelation ____ 12

2.3 Hydrogels in Bone Tissue Engineering ____ *13*

2.3.1 Classification of Hydrogels ____ **13**

2.3.3 Requirements for Hydrogel-based Biomaterial 15

2.3.4 Fibrin-based Hydrogel 16

2.3.4.1 Composition and structure of fibrin 16

2.3.4.2 Fibrin-based Hydrogel in Bone Tissue Engineering 17

2.3.4.3 Rheological properties of Fibrin Hydrogel 18

2.3.4.3 Modification of mechanical properties of Fibrin 18

Chapter 3 ***20***

Materials and Methods ***20***

3.1 Materials ***20***

3.2 Preparation of Collagen/nanohydroxyapatite Scaffolds ***20***

3.3 Fibrin-OPN Hydrogel ***20***

3.3.1 Preparation of Fibrin Hydrogel 20

3.3.2 Preparation of OPN 21

3.3.3 Preparation of Fibrin - OPN Hydrogel 21

3.4 Preparation Coll/nanoHA - Fibrin Hydrogel composite ***21***

3.5 Rheological Characterization of Coll/nanoHA Scaffold-Fibrin Hydrogel ***21***

3.5.1 Dynamic Mechanical Analysis 21

3.5.2 Viscoelasticity Analysis 22

3.5.3 Statistical Analysis 22

3.6 In vitro biological studies ***22***

3.6.1 Cell Culture 22

3.6.2 Metabolic Activity 22

3.6.3 Alkaline Phosphatase Activity 22

3.6.4 Histocytochemical Staining 23

3.6.5 Statistical Analysis 23

Chapter 4 ***24***

Results ***24***

4.1 Rheological characterization of Coll/nanoHA Scaffold-Fibrin Hydrogel ***24***

4.2.1 Dynamic Mechanical Analysis 24

4.2.1.1 Coll/nanoHA scaffolds – Fibrin Hydrogels 24

4.2.1.2 Coll/nanoHA scaffolds – Fibrin Hydrogels – OPN 27

4.2.2 Viscoelasticity Analysis 29

4.2.1.1 Fibrin Hydrogels 30

4.2.1.2 Fibrin - OPN Hydrogels 32

4.3 In vitro Biological Studies _____ *35*

4.3.1 Metabolic Activity _____ **35**

4.3.2 Alkaline Phosphatase Activity _____ **38**

4.3.3 Histocytochemical Staining _____ **39**

Chapter 5 _____ *41*

Discussion _____ *41*

Chapter 6 _____ *45*

Conclusion and Future Outlook _____ *45*

References _____ *45*

Appendix A – ALP activity for osteoblastic phenotype expression of MG63 osteoblast-like cells *50*

Appendix B – Optical In Vitro of histocytochemical staining for osteoblastic phenotype expression of MG63 osteoblast-like cells _____ *51*

LIST OF FIGURES

Figure 1: Hierarchical architecture of bone tissue from macroscopic to nanometer scale **4**

Figure 2: Bone tissue cells: osteocytes, osteoblasts, osteogenic, and osteoclasts **5**

Figure 3: Collagen type I: Hierarchical level of fibril arrangement **6**

Figure 4: Stages of bone fracture repair mechanism **7**

Figure 5: Graphic representation of elastic modulus versus compressive strength of different biomaterials and bone tissue **11**

Figure 6: Schematic representation of cryogelation technique **12**

Figure 7: Chemical structure representation of a hydrogel **13**

Figure 8: Physical crosslinking methods to produce physical hydrogels: (a) ionic interaction; (b) hydrogen bonding; (c) Hydrophobic interactions **14**

Figure 9: Chemical crosslinking methods to produce chemical hydrogels: (a) Schiff base action; (b) Diels-Alder cycloaddition; (c) Michael addition **15**

Figure 10: Structure of fibrinogen molecule **16**

Figure 11: Fibrin polymerization process, thrombin-mediated exposing the A and B knobs which leaves an A:a and B:b binding, forming the protofibrils, and subsequently their antiparallel cross-linking interaction result in a fibrin fibres **17**

Figure 12: Stress-strain curve of fibrin non-linear characteristic: (filled circles) 6 mg ml−1 human fibrinogen polymerized under coarse clotting conditions, and (open circles) 5% polyacrylamide polymerized with ammonium persulphate and tetramethylethylenediamine (TEMED) **18**

Figure 13: Storage modulus (E') of the Coll/nanoHA/Fb samples under dynamic compression solicitation versus frequency (0.1 Hz to 10 Hz) **24**

Figure 14: Storage modulus (E') of the Coll/nanoHA/Fb samples under compression solicitation with frequency of 0.1 and 10 Hz **25**

Figure 15: Loss modulus (E'') of the Coll/nanoHA/Fb samples under dynamic compression solicitation versus frequency (0.1 Hz to 10 Hz) **25**

Figure 16: Loss modulus (E'') of the Coll/nanoHA/Fb samples under compression solicitation with frequency of 0.1 and 10 Hz **26**

Figure 17: Tan δ of the samples under dynamic compression solicitation versus frequency (0.1 Hz to 10 Hz) **26**

Figure 18: Storage modulus (E') of the Coll/nanoHA_Fb 1:2 HTb samples with Low concentration (LC) and High concentration (HC), under dynamic compression solicitation versus frequency (0.1 Hz to 10 Hz) **27**

Figure 19: Storage modulus (E') of the Coll/nanoHA_Fb 1:2 HTb samples with OPN Low concentration (LC) and High concentration (HC), under compression solicitation with frequency of 0.1 and 10 Hz **28**

Figure 20: Loss modulus (E'') of the Coll/nanoHA_Fb 1:2 HTb samples with OPN Low concentration (LC) and High concentration (HC), under dynamic compression solicitation versus frequency (0.1 Hz to 10 Hz)**_____28**

Figure 21: Loss modulus (E'') of the Coll/nanoHA_Fb 1:2 HTb samples with OPN Low concentration (LC) and High concentration (HC), under compression solicitation with frequency of 0.1 and 10 Hz**_____29**

Figure 22: Tan δ of the Coll/nanoHA_Fb 1:2 HTb samples with OPN Low concentration (LC) and High concentration (HC), under dynamic compression solicitation versus frequency (0.1 Hz to 10 Hz)**_____29**

Figure 23: Storage modulus (G') of the Fb hydrogels samples under a shear stress force versus frequency (0.01 Hz to 2 Hz) **_____30**

Figure 24: Storage modulus (G') of the Fb hydrogels samples to frequency values of 0.1 Hz and 1 Hz) **_____ 30**

Figure 25: Loss modulus (G'') of the Fb hydrogels samples under a shear stress force versus frequency (0.01 Hz to 2 Hz) **_____31**

Figure 26: Loss modulus (G'') of the Fb hydrogels samples to frequency values of 0.1 Hz and 1 Hz) **_____ 31**

Figure 27: Tan δ of the samples under shear stress force versus frequency**_____32**

Figure 28: Storage modulus (G') of the Fb hydrogels with OPN Low concentration (LC) and High concentration (HC) samples under a shear stress force versus frequency (0.01 Hz to 2 Hz) **____33**

Figure 29: Storage modulus (G') of the Fb hydrogels with OPN Low concentration (LC) and High concentration (HC) samples to frequency values of 0.1 Hz and 1 Hz **_____33**

Figure 30: Loss modulus (G'') of the Fb hydrogels with OPN Low concentration (LC) and High concentration (HC) samples under a shear stress force versus frequency (0.01 Hz to 2 Hz) **_____34**

Figure 31: Loss modulus (G') of the Fb hydrogels with OPN Low concentration (LC) and High concentration (HC) samples to frequency values of 0.1 Hz and 1 Hz) **_____34**

Figure 32: Tan δ of the samples under shear stress force versus frequency **_____35**

Figure 33: Metabolic activity of MG63 cells after culture on Coll/nanoHA scaffold_Fb 1:2 HTb sample with different concentration of substrate medium /cell culture medium (only-substrate medium, 1:1 and 1:3, respectively) for 1, 3 and 6 days, estimated by Resazurin assay. The control, culture (TCPS) was considered 100% (*, significantly different comparing Fb 100 (only-substrate medium) with Fb 50 (1:1 substrate medium /cell culture medium) on the same time point (day 3), $p<0.005$); (**, significantly different comparing Fb 100 (only-substrate medium) with Fb 25 (1:3 substrate medium /cell culture medium) on the same time point (day 3), $p<0.006$); (***, significantly different comparing Fb 100 (only-substrate medium) with Fb 25 (1:3 substrate medium /cell culture medium) on the same time point (day 6), $p<0.02$) **_____36**

Figure 34: Metabolic activity of MG63 cells after culture on Coll/nanoHA scaffold_Fb 1:2 HTb_OPN LC (10 μg/mL) sample with different concentration of substrate medium /cell culture medium (only-substrate medium, 1:1 and 1:3, respectively) for 1, 3 and 6 days, estimated by Resazurin assay. the control, culture (TCPS) was considered 100% (*, significantly different comparing OPN L 50 (1:1 substrate medium/cell culture medium) with OPN LC 25 (1:3 substrate medium /cell culture medium) on the same time point (day 6), $p<0.037$) **_____36**

Figure 35: Metabolic activity of MG63 cells after culture on Coll/nanoHA_Fb 1:2 HTb_OPN HC (100 µg/mL) sample with different concentration of substrate medium /cell culture medium (only-substrate medium, 1:1 and 1:3, respectively) for 1, 3 and 6 days, estimated by Resazurin assay. the control, culture (TCPS) was considered 100% (*, significantly different comparing OPN HC 100 (only-substrate medium) with OPN HC 50 (1:1 substrate medium /cell culture medium) on the same time point (day 6), p<0.028); (**, significantly different comparing OPN HC 100 (only-substrate medium) with OPN HC 25 (1:3 substrate medium /cell culture medium) on the same time point (day 3), p<0.028); (***, significantly different comparing OPN HC 100 (only-substrate medium) with OPN HC 50 (1:1 substrate medium /cell culture medium) on the same time point (day 1), p<0.015) **37**

Figure 36: Metabolic activity of MG63 cells after culture on Coll/nanoHA_Fb 1:2 HTb, Coll/nanoHA_Fb 1:2 HTb_OPN HC (100 µg/mL) and, Coll/nanoHA_Fb 1:2 HTb_OPN LC (10 µg/mL) sample for only-substrate medium for 6 days, estimated by Resazurin assay. the control, culture (TCPS) was considered 100% **38**

Figure 37: ALP activity for osteoblastic phenotype expression of MG63 osteoblast-like cells culture for Coll/nanoHA_Fb 1:2 HTb, Coll/nanoHA_Fb 1:2 HTb_OPN HC (100 µg/mL), and Coll/nanoHA_Fb 1:2 HTb_ OPN LC (10 µg/mL) composite for only-substrate medium after culture at day **38**

Figure 38: Histomorphometric analysis for osteogenic differentiation of the MG63 cells after 6 days of culture with Fb 100, OPN HC 100, OPN LC 100 (eluate with degradation products), and TCPS samples. Von Kossa – Phosphate deposits stain. Scale: 200 µm. Red arrows evidence the ECM mineralization **39**

Figure 39: Histomorphometric analysis for osteogenic differentiation of the MG63 cells after 6 days of culture with Fb 100, OPN HC 100, OPN LC 100 (eluate with degradation products), and TCPS samples. Sirius red for type I collagen stain. Scale: 200 µm. Red arrows evidence the higher protein deposition (cell ECM) **40**

Figure 40: ALP activity for osteoblastic phenotype expression of MG63 osteoblast-like cells culture for Coll/nanoHA scaffold_Fb 1:2 HTb composite with different concentration substrate medium/ cell culture medium (only-composite, 1:1 and 1:3) after culture at day 6 **50**

Figure 41: ALP activity for osteoblastic phenotype expression of MG63 osteoblast-like cells culture for Coll/nanoHA_Fb 1:2 HTb_OPN LC (10 µg/mL) composite with different concentration substrate medium/ cell culture medium (only-composite, 1:1 and 1:3) after culture at day 6 **50**

Figure 42: ALP activity for osteoblastic phenotype expression of MG63 osteoblast-like cells culture for Coll/nanoHA_Fb 1:2 HTb_OPN HC (100 µg/mL) composite with different concentration substrate medium/ cell culture medium (only-composite, 1:1 and 1:3) after culture at day 6 **50**

Figure 43: Histomorphometric analysis for osteogenic differentiation of the MG63 cells after 1, 3 and 6 days of culture with Fb 100, OPN HC 100, OPN LC 100 (eluate with degradation products), and TCPS samples. Sirius red for type I collagen stain. Scale: 200 µm **51**

Figure 44: Histomorphometric analysis for osteogenic differentiation of the MG63 cells after 1, 3 and 6 days of culture with Fb 50, OPN HC 50, OPN LC 50 (eluate with degradation products), and TCPS samples. Sirius red for type I collagen stain. Scale: 200 µm **52**

Figure 45: Histomorphometric analysis for osteogenic differentiation of the MG63 cells after 1, 3 and 6 days of culture with Fb 25, OPN HC 25, OPN LC 25 (eluate with degradation products), and

TCPS samples. Sirius red for type I collagen stain. Scale: 200 µm **53**

Figure 46: Histomorphometric analysis for osteogenic differentiation of the MG63 cells after 1, 3 and 6 days of culture with Fb 100, OPN HC 100, OPN LC 100 (eluate with degradation products), and TCPS samples. Von Kossa – Phosphate deposits stain. Scale: 200 µm **54**

Figure 47: Histomorphometric analysis for osteogenic differentiation of the MG63 cells after 1, 3 and 6 days of culture with Fb 50, OPN HC 50, OPN LC 50 (eluate with degradation products), and TCPS samples. Von Kossa – Phosphate deposits stain. Scale: 200 µm **55**

Figure 48: Histomorphometric analysis for osteogenic differentiation of the MG63 cells after 1, 3 and 6 days of culture with Fb 25, OPN HC 25, OPN LC 25 (eluate with degradation products), and TCPS samples. Von Kossa – Phosphate deposits stain. Scale: 200 µm **56**

LIST OF TABLES

Table 1: Structural/Biological Variables of variation of fibrinogen and thrombin concentrations_____**19**

LIST OF ABBREVIATIONS

3D	three-dimensional
ALP	Alkaline phosphatase
BMPs	bone morphogenetic proteins
BGs	bioactive glasses
Coll	collagen
ECM	extracellular matrix
EDC	1-ethyl-3-(3-dimethyl aminopropyl) carbodiimide hydrochloride
Fb	fibrin
HA	hydroxyapatite
HTb	high thrombin concentration
HC	high concentration
LC	low concentration
LTb	low thrombin concentration
nanoHA	nanohydroxyapatite
NHI	national institute of health
NHS	n-hydroxysuccinimide
OPN	osteopontin
PAA	poly(acrylic acid)
PAAm	poly(acrylamide)
PBS	phosphate buffered saline
PCL	poly(caprolactone)
PEG	poly(ethylene glycol)
PGA	poly(glycolic acid)
PHEMA	poly(hydroxyethyl methacrylate)
PVA	poly(vinyl alcohol)
PLA	poly(lactic acid

RGD	arg-gly-asp
ß-TCP	beta- tricalcium phosphate
Tb	thrombin
TBS	tris-phosphate buffered saline
TCP	tricalcium phosphate

Chapter 1

Objectives and Document Structure

1.1 Objectives of the work

This master thesis work aims to develop a 3D Coll/nanoHA scaffold containing Fb hydrogel incorporations in order to improve the mechanical properties of the graft and augment the regenerative properties of bone tissue. In addition, the Fb hydrogel was conjugated with pro-regenerative recombinant protein such as osteopontin (OPN).

Biomechanical properties of the composite (Coll/nanoHA scaffold + Fb Hydrogel with/without OPN) were evaluated by DMA assay (Storage Modulus, Loss Modulus, Loss Factor). The viscoelasticity of Fibrin hydrogel and Fibrin hydrogel + OPN (10 µg/mL (LC) or 100 µg/mL (HC)) was evaluated by rheometer analysis (Storage Modulus, Loss Modulus). The fibrin hydrogel network was tuneable varying the fibrinogen/thrombin concentrations to achieve the optimal mechanical properties. In this study, four different hydrogels were analysed, presenting the follow concentration of fibrin and thrombin, respectively:

- Fb 1:1 LTb (10 mg/ml and 1 NHI (U/mL)).
- Fb 1:1 HTb (10 mg/ml and 3.5 NHI (U/mL)).
- Fb 1:2 LTb (6.3 mg/ml and 1 NHI (U/mL)).
- Fb 1:2 HTb (6.3 mg/ml and 2 NHI (U/mL)).

Biological characterizations of the composite materials degradation products with the optimal content of the Fb/Tb were analysed by *in vitro*-assays standard cell line (MG63). The metabolic activity of the cells was measured by Alamar blue assay and the osteoblast differentiation by cellular alkaline phosphatase (ALP) activity. Subsequently, histocytochemical staining was performed to evaluate the type I Collagen and Calcium Phosphate deposits with the time in culture (1, 2, and 6 days) by Inverted Optical microscopy.

1.2 Document structure

This master thesis is organized into chapters. Chapter 2 addresses the literature review, and the state of the art. Chapter 3 approaches the methodology applied in this work, describing the mechanical, physic, and chemical characterization of the materials in the study. Chapter 4 presents the results obtained, and in chapter 5 their suitable discussion. Finally, chapter 6 presents the conclusions and future perspectives of the work developed.

Chapter 2

Literature Review

2.1 Introduction

Tissue engineering is a multidisciplinary field of science that focuses on providing alternative strategies for the treatment of organ/tissue defects. The combination of materials science, engineering principles, and biomedical engineering allows the fabrication of composite constructs, providing the repair or replacement of damaged tissue avoiding undesirable inflammatory responses [1].

Clinical solutions for bone repair include autographs, allographs, and xenografts. Autographs are the "gold standard" for the repair of bone defects. This therapy uses the bone from the same individual that receives the implant. Therefore, autografts have a low risk of bone graft rejections and are biocompatible and non-immunogenic. Although, this bone graft transplant may result in a donor site injury and increase patient morbidity. Allografts and xenografts use the bone of the same species and different species, respectively, for the repair of the bone defect. These alternative solutions have some limitations associated with the rejection or transmission of diseases and have lower tissue properties as compared with autografts. In addition to these disadvantages, xenografts can also carry the risk of transmission of zoonotic diseases (e.g., Rabies, Brucellosis, Plague, or Salmonella*)* [2, 3].

Hence, bone tissue engineering is a potential strategy compared to conventional techniques. The field of bone tissue engineering achieves the repair of bone pathologies without the problems associated with conventional therapies and improves graft incorporation, osteogenicity, osteoconductivity, and osteoinductivity [3, 4]. Bone tissue engineering aims to support cell adhesion, migration, and proliferation and promote the growth of new functional tissue rather than just implanting non-living scaffolds. Typically, there are three groups of biomaterials to produce scaffolds in tissue engineering: ceramics, synthetic polymers, and natural polymers. Collagen (Coll) is a natural polymer and hydroxyapatite (HA) is a bioceramic. These two materials are successfully applied in tissue engineering due to their high interaction with bone cells, which enhance cell adhesion and proliferation [5]. Polymer materials such as hydrogels have several potential advantages in bone tissue repair. Their three-dimensional (3D) hydrophilic polymer chains provide a nutrient environment suitable for endogenous cell growth. Therefore, the network structure of the hydrogels presents a prospective ability to encapsulate bioactive molecules or cells, allowing this material to act as a delivery vehicle [6].

2.2 Bone

2.2.1 Function

The human skeletal system presents more than 200 bones divided into different types based on shape and function (e.g., long, short, flat, and irregular bones). Bones are the main mechanical support of the human skeletal system with the ability to perform a wide array of functions. Bone locomotion, load-bearing capacity, protection of internal organs, provision of biological elements to hematopoiesis, and maintain the homeostasis of key electrolytes by calcium and phosphate ion storage are some of the functions that bone provides [2].

2.2.2 Structure

Bone is described as a dense connective tissue with an irregular but the optimized arrangement, being a heterogeneous and anisotropic material. The bone structure is made up of different types of living cells dispersed in a mineralized extracellular matrix, which ranges by different scales (Fig. 1)[7, 8].

At the macroscopic level, bone presents two different architectural structures: trabecular or cancellous bone (20% of the total bone skeleton) and cortical or compact bone (80% of the total bone skeleton). Cortical bone is characterized for show a dense structure with 10% porosity and having lower blood vessel concentration when compared to trabecular bone. Thus, trabecular bone shows high porosity (50-90%) and higher vascularization. At the microstructural level ((from 10 to 500 μm) compact bone is composed mainly of osteon and Haversian system units, which act as weight-bearing pillars. On the other hand, trabecular bone consists of a reticular structure of bars, plates, and rods of various sizes called trabeculae. At the nanostructural level (from 10 to 1000 nm) bone is made up mainly of collagen fibres and nanocrystals of bone minerals, mostly nanohydroxyapatite [8].

The mechanical, biological, and chemical properties of bone depend on the different architectural structures. Typically, the tensile strength of trabecular bone is approximately 7.4 MPa, compressive strength ranges from 4-12 MPa, and Young's modulus 0.02-0.05 GPa. Therefore, cortical bone is described as a dense and low porous structure. Thus, this bone structure shows a higher mechanical response compared to trabecular bone. Generally, cortical bone presents a tensile strength range of 60-160 MPa, compressive strength range of 130-180 MPa, and Young's modulus between 3-30 GPa [9].

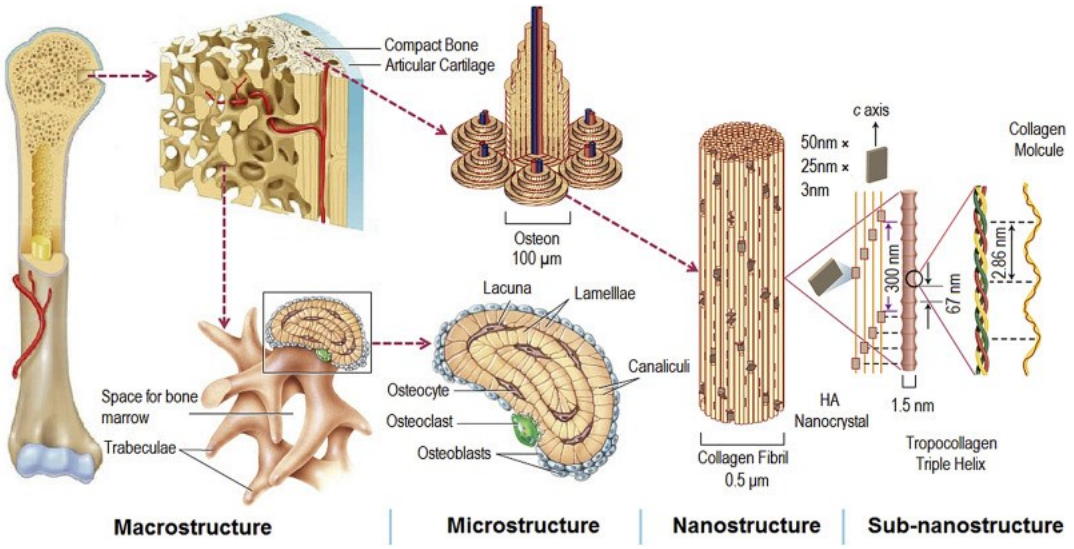


Figure 1 – Hierarchical architecture of bone tissue from macroscopic to nanometer scale [8].

2.2.3 Constitution

Mammalian bone contains about 30% organic and 70% inorganic segments. The inorganic phase presents approximately 90% collagen, and 10% non-collagenous proteins, lipids, proteoglycan molecules, osteopontin (OPN), and other bone matrix proteins. The mineral phase of bone (organic phase) is mainly HA nanocrystals. Water is also a constituent of bone structure, range 5 to 10 % of the total bone composition. Bone matrix proteins play a key role in mechanical strength and tissue adhesive characteristics. Therefore, the bone extracellular matrix (ECM) is composed of an inorganic phase (predominantly Coll) which provides mechanical resilience, and mineralised elements (e.g., HA) that deliver stiffness resistance to the bone and are an accessible reservoir of mineral ions [7, 10].

The regulation of these extracellular components is achieved by bone cells: osteogenic, osteoblasts, osteocytes, and osteoclasts (Fig. 2). Each bone cell is critical to bone function. Osteoblasts are specialised fibroblast-like cells and are derived from osteoprogenitor cells of mesenchymal origin in bone marrow (i.e., pluripotent mesenchymal stem cells) and other connective tissues. The main function of osteoblast cells in the production of ECM bone components (e.g., type I collagen, proteoglycans, non-collagenous, and cell attachment proteins). For this reason, they are responsible for the growing or remodelling of bone. Osteoblast differentiation and proliferation occurred before bone formation and are stimulated by bone morphogenetic proteins (BMPs). When maturated they can be converted to a layer of cuboidal cells, which can undergo apoptosis or become osteocytes and bone-lining cells [7, 11]. Osteocytes are derived from mesenchymal stem cells (MSCs). They are characterized by showing a star-like morphology and for be the most abundant cell type of bone. The principal function of osteocyte cells is to coordinate the activity of osteoclasts and osteoblasts bone cells by detecting the need for bone augmentation or reduction. Consequently, they are vital to bone cell tissue communication [7, 12]. Osteoclasts are derived from the hematopoietic lineage. These cells resorb bone by realising enzymes and acids. Thus, osteoclasts are important in the bone remodelling process, responding to changes in mechanical stress in the skeleton. During the activity of

osteoclasts is formed at bone surface depressions known as Howship's lacunae. This helps the creation of new pathways for nerves and vessels to grow through the bone and provide new bone formation. Finally, bone lining cells are described as inactive flat-shaped osteoblasts. These cells cover the bone surface and are important in the bone remodelling process, in mineral hematopoiesis, and osteoclastic differentiation [7, 11].

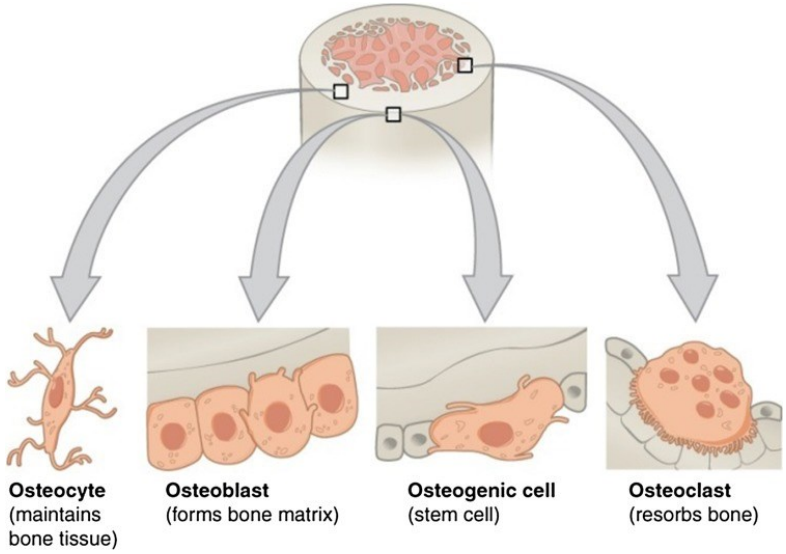


Figure 2 – Bone tissue cells: osteocytes, osteoblasts, osteogenic, and osteoclasts [7].

2.2.3.1 Collagen

Type I Collagen is the most abundant protein in the mammalian´s bone representing approximately 95% of the entire collagen content of bone. This protein present in the bone inorganic phase is responsible for maintaining its structural integrity. In bone, collagen fibrils are arranged in concentric waves (Fig. 3), enable the capacity to resist tensile, shear, or compression forces. Collagen fibrils are characterized for present high-aspect-ratio polypeptides, tropocollagen molecules, with triple helix (300 nm in length and 1.5 nm in diameter). The multiple combinations of collagen microfibrils make up the collagen fiber. Mechanically collagen is characterized for showing a tensile strength between 0.9-1.4 MPa and Young's modulus between 0.0018-0.046 GPa. The gap regions performed in fibril cross-linking molecules in bone are filled by HA crystals, increasing collagen protein stiffness [13-15].

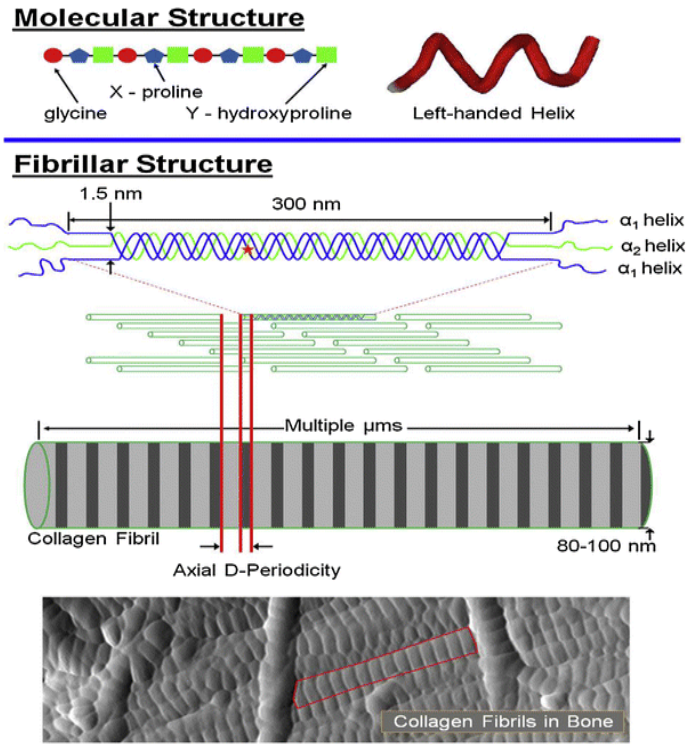


Figure 3 – Type I Collagen: hierarchical level of fibril arrangement [13].

2.2.3.2 Nanohydroxyapatite

Hydroxyapatite ($Ca_{10}(PO_4)_6(OH)_2$) is the main mineral present in a mammal's bone skeleton. In bone, HA is constituted by apatite platelets with a thickness of 2–7 nm, length of 15–200 nm, and width of 10–80 nm. The growth of HA crystals occurs within collagen fibrils. For this reason, Coll fibrils play a key role in triggering nucleation and modulating HA particles. The formation of HA particles is named as mineralization process. This process occurs in two different stages: primary mineralization and second mineralization. In the first mineralization phase, HA particles grow rapidly being limited by surrounding collagen fibrils, and an intense ionic exchange happens between HA mineral particles and surrounding biological fluid. Because of this, natural HA found in human bone is non-stoichiometric with a Ca/P ratio of less than 1.67. In the second mineralization phase, the ionic exchange decreases, and the thickness of HA crystals increase. Mechanically, this calcium phosphate ceramic is characterized by presenting a tensile strength between 21-60 MPa and Young's modulus between 70-120 GPa [16-18].

2.2.4 Bone Repair Process

The bone tissue has the capacity to repair itself after a fracture. A bone fracture is described as a gap in the bone structure, presenting different types and severities. Bone fracture regeneration can be divided into four stages: Hematoma formation, Fibrocartilaginous callus formation, Bony callus formation, and Bone remodelling. Immediately after a bone fracture, a hematoma is formed. The sequence of bone repair is displayed in figure 4. In this process, the blood is released from broken or torn vessels, which results in coagulation of blood and an acute inflammatory response. Thus, blood clot acts as a temporary scaffold, crucial for primary

fundamental strength and basis of new bone formation. Once the blood coagulation is formed, the bone repair is initiated. Hence, the hematoma is replaced by fibres (soft tissue). This phase is denominated as fibrocartilaginous callus formation, providing mechanical support to the fracture site. Subsequently, the soft callus is switched with a hard bone, identified as a bony callus. In this stage, an intense osteoblast activity will provide the new bone matrix formation. Bone remodelling is the final phase when the woven bone is converted into a dense bone at the centre of the bony callus. Progressively, a bony callus is replaced by a compact bone in the tissue edges and a lamellar bone in the middle. So, the bone recovers the original structure as soon as the blood circulation in the area progresses [7, 19, 20].

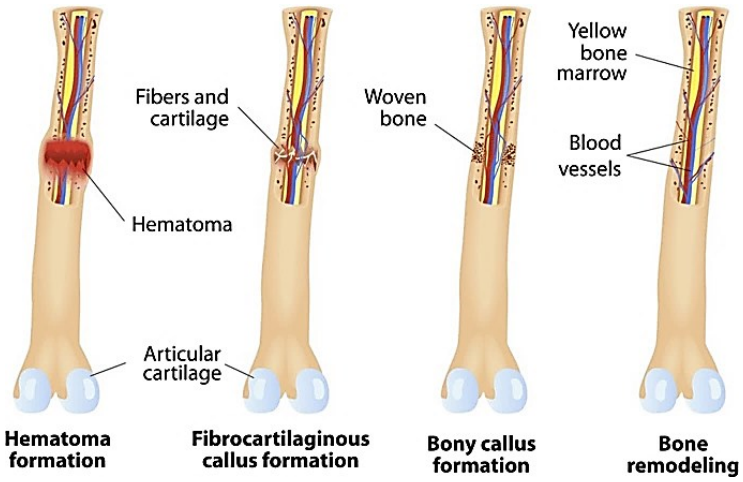


Figure 4 – Stages of bone fracture repair mechanism [7].

2.2.4.1 Osteopontin in Bone Repair

Osteopontin is a non-collagenous protein, representing 1-2% of bone non-collagenous proteins. OPN is a highly charged and phosphorylated protein showing a high affinity to calcium. For this reason, this protein can regulate the bone mineral phase, controlling the nucleation, growth, shape, and size of HA crystals. Besides, the high network of phosphorylated amino acids presented in the OPN structure is crucial to the properties of the bone extracellular matrix, allowing the dissipation of large amounts of energy when exposed to a stress force. At the bone biomineralization stage, OPN plays a key role in the modulation of osteoblasts, osteoclastic function, and matrix mineralization. Thus, the increase of OPN concentration in the collagen matrix increases the adhesion of osteoblast and osteoclast cells [21-23].

2.2 Bone Tissue Engineering

Tissue engineering arise from the necessity to repair missing or malfunctioning human tissues. Biomaterials constructs such as 3D scaffolds play a key role in engineering tissues, being crucial to mimic the bone ECM structure. These biomaterials serve as a template structure for tissue regeneration, promoting cell seeding, proliferation, and new tissue formation. Thus, these biomaterials offer a potential solution to overcome the current problems of replacing lost tissue function and boost neovascularization and bone regeneration. To achieve proper vascularization and host tissue integration, biocomposite materials based on Coll and nanoHA are widely applied in bone tissue engineering [2, 24].

2.2.1 Scaffolds

Scaffold's biomaterials can be described as a 3D porous structure that is capable to promote cellular proliferation, as well as supplying nutrients, oxygen, removal of the products of cellular metabolism, and controlled delivery of molecules of interest (drugs and growth factors). There are several key important requirements that scaffolds should follow to promote higher pro-regenerative tissue response. Below is described some important properties when designing or producing a scaffold for tissue engineering application [25].

I. Biocompatibility

Biocompatibility is one of the most important requirements in the selection of scaffold materials. The scaffold should replace the damage/loss of body tissue, so it must support normal cellular function (attachment, proliferation, migration, and differentiation). After implantation, the scaffold should prevent severe inflammatory responses that might reduce healing or cause rejection by the body. Thus, biocompatibility is crucial to promote new bone tissue growth successfully in a satisfactory environment without cytotoxicity problems [25].

II. Biodegradability

Tissue engineering aims to provide a scaffold that acts as a cell delivery vehicle and not only replaces the damaged/dysfunctional tissue with a permanent biomaterial. Consequently, the scaffold must be biodegradable allowing the body's cells to replace the implanted scaffold by producing their own ECM. Therefore, the degradation rate of the scaffold should be similar to the tissue formation. Polymers such as, polylactic acid, polyglycolic acid, and polycaprolactone, are biomaterials that have an adaptable degradation rate, so they are commonly used in scaffolds for tissue regeneration. The degradation rate is directly linked to chemical factors such as polymeric composition, molecular weight, crystallinity, and scaffolding techniques. The degradation products of the material must be non-toxic and be able to be excreted from the body without causing damage to other organs or tissues[18, 25].

III. Pore size

The scaffold architecture is of critical importance once the interconnective structure and porosity allow cell migration and nutrients transport within the construct and to the extracellular matrix formed by these cells. For this reason, the structure of the scaffold should provide high cellular migration, proliferation, and differentiation. Therefore, pore size should be within the

critical range: needs to be large enough to improve cell migration within the scaffold's structure but must be small enough to provide a high specific surface. Studies have shown that the scaffold's pore size range should have a bimodal distribution (micro- and macroporous). For bone tissue, scaffolds should be between 100 and 500 μm to achieve optimal cell attachment without compromise the mechanical properties of the graft [18, 25].

IV. Mechanical properties

Producing scaffolds with sufficient mechanical integrity is crucial once the scaffolds should be strong enough to handle surgical implantation and function from the time of implantation to the completion of the repairing process. Ideally, the mechanical properties of the scaffold should be similar to the damages and/or dysfunctional tissue to require a desired biological response. Once the repair rate in young individuals is different than in elder individuals this is too must be considered when designing scaffolds. As the healing time is longer in elder patients, the material needs to have a lower degradation rate and higher mechanical integrity. Therefore, to provide successful scaffold implantation should be a balance between mechanical properties and porous architecture to allow cell migration, proliferation, and vascularization [25].

2.2.2 Biomaterials

Typically, in the field of bone tissue engineering, materials such as natural polymers (such as collagen, gelatin, silk fibroin, and chitosan), synthetic polymers (such as Poly (lactic acid) (PLA), Poly(glycolic acid) (PGA), and Poly(caprolactone) (PCL)), ceramics (such as HA, beta-tricalcium phosphate (β-TCP), and bioactive glasses (BGs)), and their composites are used to produce scaffolds. Usually, metals present a much higher mechanical strength than natural bone, causing stress shielding (i.e., mechanical bypass of loads around the implant) which can result in bone resorption. However, metals such as titanium, tantalum, and their alloys are considered mechanically preferential biomaterials for scaffolds. These metals present similar mechanical properties to the natural bone, which improve bone ingrowth. However, these metals show a non-biodegradable behaviour, leaving the need for additional surgery, and also had high-cost manufacturing, becoming their development less attractive in this field of engineering. The choice of material for bone scaffold applications is an important first criterion. To guarantee the success of the material chosen, this should present mechanical properties close to the natural bone and be suitable to be applied in medical applications. Each group of materials presents advantages and disadvantages. Ceramic materials have been widely used for scaffold bone regeneration applications due to their outstanding mechanical properties, excellent biocompatibility, thermal stability, and corrosion resistance. Natural polymers are mainly proteins (e.g., collagen) with bio-functional molecules that guarantee bioactivity. Although, these materials showed a reduced tunability, uncontrollable degradation rate, and weak mechanical strength. Thus, the combination of polymers materials with bioceramics allows the combination of higher biological response and mechanical properties to the scaffolds, which are superior characteristics for the manufacturing of scaffolds for bone tissue engineering [24, 25].

2.2.1.1 Bioceramics

Ceramic materials are characterized for posing a high mechanical stiffness (Young's modulus) and very low elasticity. Ceramics such as HA, tricalcium phosphate (TCP), ß-TCP, and BGs are the most common materials applied for ceramic scaffolds. These materials show excellent biocompatibility with chemical and structural similarity to the mineral phase of native bone. Thus, osteoblast differentiation and proliferation are favoured, and enhancing tissue regeneration [24, 25].

In bone natural ECM the constituents are nanometres in diameter and at the molecular level (proteins, lipids, carbohydrates, and nucleic acids) are governed by their nanoscale sizes, patterns, and folding. Therefore, the presence of synthetic nanoHA in scaffolds is extremely advantageous since the bone has in its natural structure nanoHA. HA can be characterized as a non-toxic compound, highly biocompatible, and bioactive (induces bone tissue regeneration) [26]. The nanometre grain size of nanoHA enhances osteoblast's metabolism and enables higher adhesion, proliferation, and differentiation of progenitor cells. The natural hydroxyapatite found in bone tissue is non-stoichiometric and is deficient in ions such as calcium (Ca) and phosphate (P). Other ions as Na^{+}, Mg^{2+}, and Al^{3+} can be found as a substitute for Ca position when compared with synthetic HA. In addition, carbonate ions (CO_3^{2-}) can substitute phosphate elements. On the other hand, artificial HA has a stoichiometric Ca/P molar ratio of 1.67. There are some significant differences between synthetic and biological hydroxyapatite. Thus, the morphology, stoichiometry, crystallinity, and phase purity of artificial HA are crucial for its mechanical properties and bioactivity as a scaffold for tissue regeneration [17, 25].

2.2.1.2 Polymers

Polymer materials can be divided into two different groups: natural polymers and synthetic polymers. Usually, natural polymers such as silk fibroin, collagen, gelatin, fibrin, elastin, cellulose, alginate, dextran, starch, chitin/chitosan, glycosaminoglycans, hyaluronic acid are the most used as biomaterials in scaffolds. Synthetic polymers such as PLA, PGA, PCL, polylactide-co-glycolide (PLGA), polyanhydrides, polycarbonates, polyphosphazene, polyurethanes, and polypropylene fumarate are the most common used as scaffolds materials. Natural polymers scaffolds, when compared with synthetic polymers scaffolds, exhibit a higher biological active behaviour, promoting excellent cell adhesion and growth. On the other hand, synthetic polymers show superior mechanical properties and degradation control rates. For this reason, these polymer materials are extremely used as scaffolds biomaterials for biomedical applications [8, 25].

Collagen is a natural polymer that naturally possesses chemical groups (ligands) in the form of Arg-Gly-Asp (RGD) binding sequences. These ligands are surface binding sites for cells, allowing their attachment to the substrate surface. This natural polymer can also be characterized as a material that does not induce a significant chronic inflammatory response. Since natural bone present in its structure collagen fibres, the incorporation of this natural polymer in scaffolds is particularly advantageous [2, 25].

2.2.3 Polymer/Bioceramic Scaffolds

To improve the mechanical and biological characteristics of the scaffold, achieving the ideal requirements needed, two or more materials can be combined into a scaffold. The scaffold aims to provide a temporary structure at the defect site, with sufficient mechanical integrity to support the tissue growth. To match the mechanical demands of the defect site, the mechanical characteristics of materials used in scaffolds should be similar to the natural bone tissue. Figure 5 shows the elastic modulus versus compressive strength values of different biomaterials comparatively to human bone tissue properties. Thus, polymers/ceramics composites could mimic the natural bone mechanical properties. As Coll and nanoHA are an integral part of inorganic and organic phases of bone structure, favour their use as a composite scaffold. Dense ceramics (nanoHA) shows an elastic modulus and compressive strength similar to human cortical bone but possess a brittle behaviour and a slow degradation rate. Although, biodegradable polymers (Coll) present a similar mechanical behaviour to the human cancellous bone and a tuneable degradation rate. Besides, the composite Coll/nanoHA scaffold can show osteoinduction properties without chronic inflammatory response, providing permeability for cell invasion and vascularization, and support load-bearing forces. For this reason, this polymer/bioceramic composite favour the bone tissue engineering application, responding to the mechanical and physiologic demands of the host tissue, offering a better solution for clinical demands of bone defects [2, 8].

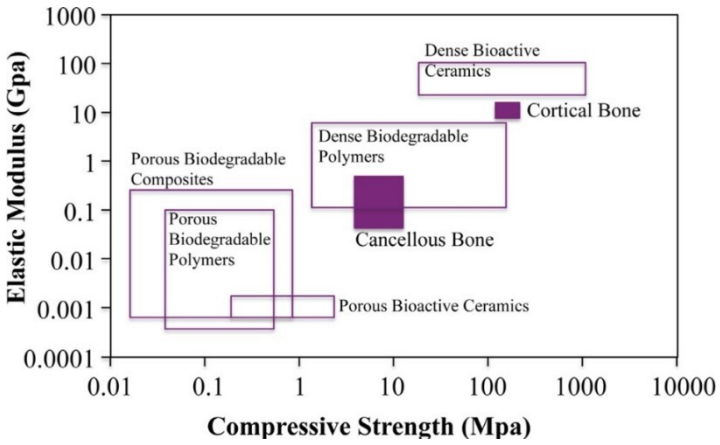


Figure 5 – Image representation of the elastic modulus versus compressive strength for different biomaterials and bone tissue constituents [2].

2.2.4 Scaffolds Production Techniques

The production technique is crucial to achieving the suitable combination of functional properties to match the replaced tissue. Obtaining a 3D scaffold construct with optimized porosity, pore size, and mechanical properties presents a challenge. The design of the construct obtained is directly linked to the cell's function within the scaffold, and subsequently with the higher capacity of new bone tissue regeneration. Conventional techniques (e.g., phase separation, solvent casting/particulate leaching, freeze-drying, and gas foaming) and advanced techniques (e.g., electrospinning, fused deposition modelling, selective laser sintering, and 3D printing) are some available strategies to produce scaffold applied in bone tissue engineering [8, 27]. Polymeric/bioceramic porous scaffolds as Coll/nanoHA scaffold can be successfully prepared by freeze-drying technique. In this technique, freezing temperatures are applied to a polymer

dissolved in an adequate water solvent, forcing the polymer molecules to aggregate into the interstitial spaces. Subsequently, the solvent is removed by sublimation. When the solvent is completely removed a dry polymer scaffold with interconnected porosity remains. This is a simple technique widely applied for bone tissue application showing higher tissue interaction, allowing cell growth and nutrient supply. Therefore, the disadvantages associated with this process are longer production time, high energy-consuming, and formation of close pores by gas foaming [28].

2.3.4.1 Cryogelation

Cryogel technology (Fig. 6) is a simple one-step process that follows the same principles of synthesis of freeze-drying technique. Cryogelation technique is described as a simple method to obtain microporous scaffolds, applying freezing temperatures 10º below to the crystallization point of the pure solvent. As solvent freezes, two different phases are formed: frozen phase and "unfrozen-liquid microphase". At the "unfrozen-liquid microphase" the polymer concentrates are dissolved and undergo cross-linking reactions. After finishing cross-linking reactions, the polymer starts to thaw. An interconnected polymeric network remains after the melting of ice crystals [29].

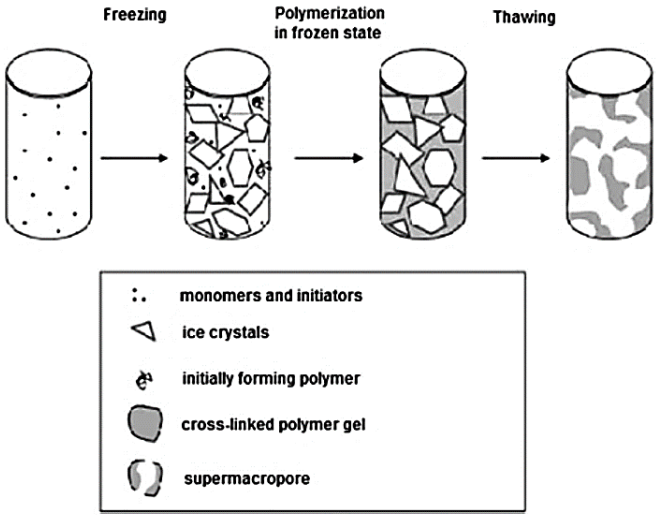


Figure 6 - Schematic representation of cryogelation technique [29].

2.3 Hydrogels in Bone Tissue Engineering

Hydrogels are described as polymeric material with a 3D hydrophilic polymer chains network and a water content of over 90%, similar to bone tissue. Figure 7 shows the chemical structural of a hydrogel. The polymeric chains are cross-linked by chemical or physical bonding, forming bridges. Between this solid polymer linked together, there are void spaces filled by a solvent, usually water. At the swollen state, the chemical and physical crosslinking points keep the 3D structure. The presence of hydrophilic groups such –NH_2, –COOH, –OH, –$CONH_2$, -CONH–, and –SO_3H are responsible for the hydrophilicity network [6, 30].

In the bone tissue engineering field, hydrogels have been widely used as vehicle for cells and drug delivery to promote higher bone regeneration. Hydrogel's characteristics: swelling/deswelling behaviour, high environmental sensitivity, high ionic conductivity, high permeability, surface properties, mechanical properties, and sorption capacity, provide an ideal environment for potential solutions in bone tissue engineering. Their natural hydrophilic 3D structure is crucial to support new bone growth (i.e., suitable environment for cell seeding and encapsulation). Besides, hydrogel's biocompatibility, biodegradability, and similar mechanical properties and structural properties to the natural bone ECM, become their development in tissue engineering highly important [6, 30, 31].

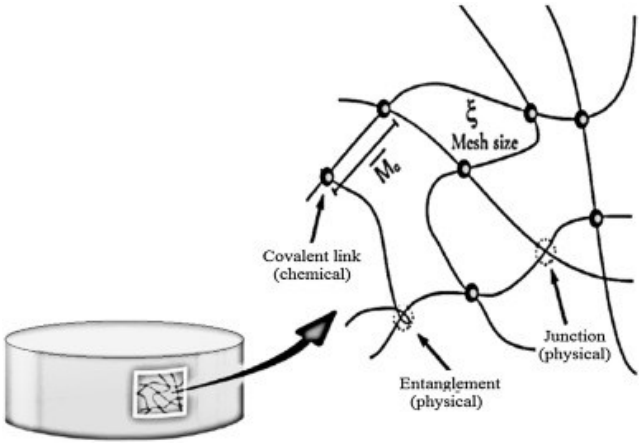


Figure 7 – Chemical structure representation of a hydrogel [30].

2.3.1 Classification of Hydrogels

Hydrogels can be classified regarding their physical properties, nature of swelling, method of preparation, network electrical charge, sources, rate of biodegradation, and nature of cross-linked bounding. Natural materials include natural proteins such as fibrin, fibroin, collagen, and alginate, and polysaccharides such as chitosan, alginate, and hyaluronic acid. These materials show high biocompatibility, low immune response and cytotoxicity, and similar structures to the native bone. Thus, these natural materials can successfully promote cell adhesion, proliferation, and differentiation. However, these biomaterials have poor mechanical strength and stability. To improve the mechanical properties, physical or chemical methods (i.e., crosslinking, and/or

copolymerization) can be applied to promote hydrogen bonding, electrostatic interaction, and internal specific functional groups. Synthetic materials as hydrogels are important for delivering active proteins, growth factors, and drugs to bone tissue. These materials when compared to natural biomaterials present lower biocompatibility and biological activity. However, their characteristics i.e., porosity, degradation time, and mechanical properties can be adjusted for the specific application. To increase biological activity synthetic materials can be combined with biological and chemical clues [30, 32, 33].

In bone tissue engineering, injectable biomaterials have been attracted special attention because of their minimally invasive injection method with the desired shape. Injectable hydrogels can be produced by physical and chemical methods. In physical methods hydrogels are formed by physical interactions, being weak secondary forces linking together different polymer chains. This method has the advantage to be easier to produce and does not require any crosslinking agents. Ionic interactions, electrostatic interactions, hydrophobic interactions, crystallization, and hydrogen bonding are the different methods to synthesize physical hydrogels, shown in figure 8. Biomaterials produced by the physical reaction can respond to changes in temperature, pH, or ionic concentration. In chemical methods, covalent bonds link together the polymer chains. Hydrogels formed by this method are insoluble in any solvents until cross-linked reaction being cleaved. Chemically cross-linked hydrogels show high mechanical strength due to their chemical bonds, enhancing the degradation time. Chemical reaction, when compared to physical methods, can achieve hydrogels with higher stability, due to the control of the flexibility and spatiotemporal of the crosslinking process. Enzymatic crosslinking, Schiff base crosslinking Michael additions, click chemistry, and photo-crosslinking are the different chemical reactions that can be used to produce chemical hydrogels, represented in figure 9 [6, 32-34]

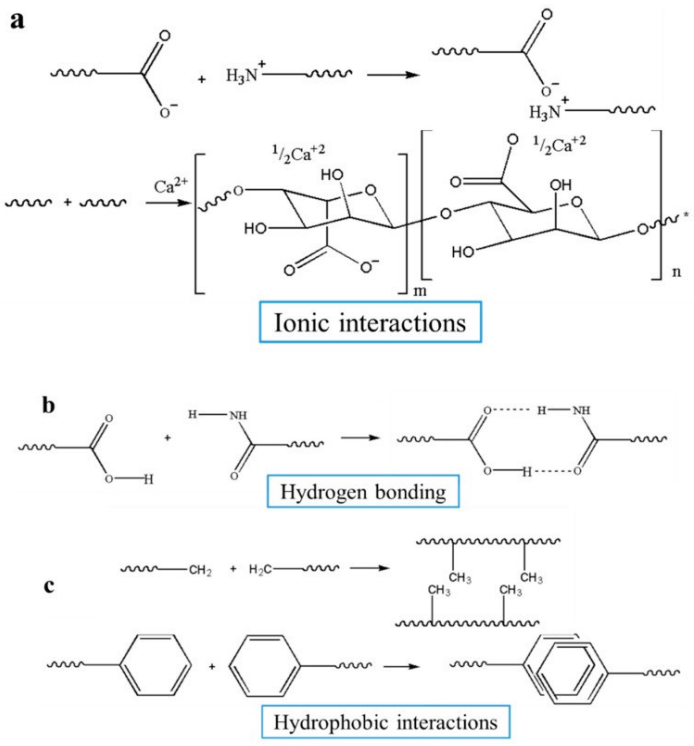


Figure 8 – Physical crosslinking methods to produce physical hydrogels: (a) ionic interaction; (b) hydrogen bonding; (c) Hydrophobic interactions [33].

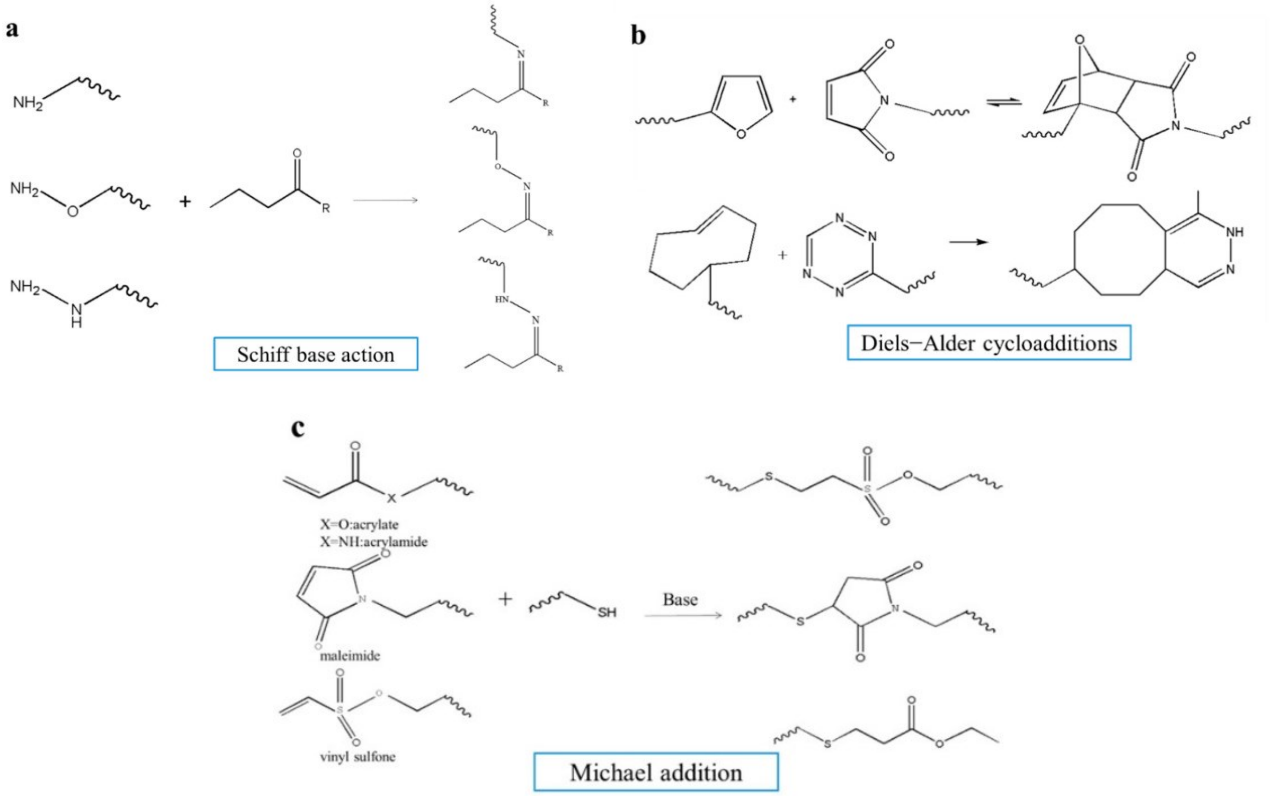


Figure 9 - Chemical crosslinking methods to produce chemical hydrogels: (a) Schiff base action; (b) Diels-Alder cycloaddition; (c) Michael addition [33].

2.3.3 Requirements for Hydrogel-based Biomaterial

The biomaterials applied to produce hydrogels should comply with several requirements. Ideally, the hydrogels for bone tissue engineering should present:

- Noncytotoxic and nonimmunogenic behaviour.
- Osteoinductive, osteoconductive, and osteogenic properties to enhance bone repair.
- Biodegradability by endogenous enzymes or hydrolysis at the same rate as the new bone tissue is formed.
- Biocompatibility of degradation products.
- High structural stability and mechanical strength to fill load-bearing defects.
- Optimal pore size and porosity to enhance normal cell function and interaction within the hydrogel structure.
- Injectable capability.

The viscoelastic behaviour of hydrogels has a direct relation to the different cellular activities. High-concentrated gels show a dense network, decreasing cell migration and ingrowth within the 3D matrix of the hydrogel. On the other hand, low-concentrated gels show a fluid network structure with lower mechanical properties, which can easily collapse during implantation. Injectable hydrogel as load-bearing scaffolds is mostly applied for filling and delivery clues due to their lower mechanical strength. However, their properties for tissue engineering application showed several advantages such as *in situ* gelling system and high biocompatibility. Hence, their development attracts special attention [6, 35].

2.3.4 Fibrin-based Hydrogel

Fibrin is described as natural biopolymer showing unique physical and biological properties, becoming their application in tissue engineering field highly advantageous. This fibrous protein is a major component of the blood clotting cascade process, being critical in wound healing repair. Thus, their 3D network performs the first scaffold for cells immediately after an injury occurs. In addition, fibrin performance excellent biocompatibility, contain specific bonding sites for membrane receptors of cell surface, promoting cell migration, fibroblast proliferation, and angiogenesis. Fibrin-based hydrogels also have the advantage of being fully injectable. However, this fibrin hydrogel presents a major disadvantage related to its lower mechanical properties. Due to rapid enzyme degradation, an uncontrollable decrease of mechanical rigidity should occur [34, 36, 37].

2.3.4.1 Composition and structure of fibrin

Fibrinogen is a soluble glycoprotein 340 kDa macromolecule present naturally in the plasma of blood. Its structure is composed of two sets of polypeptide chains, with each set presents three different peptide chains: Aα, Bß, and γ. The two sets of the polypeptide chain are connected by 29 disulphide bridges, and the three different peptide chains (Aα, Bß, and γ) are covalently linked by five disulphide bridges in the N-terminal at the central domain of the molecule (E domain), as shown in figure 10 [36, 37].

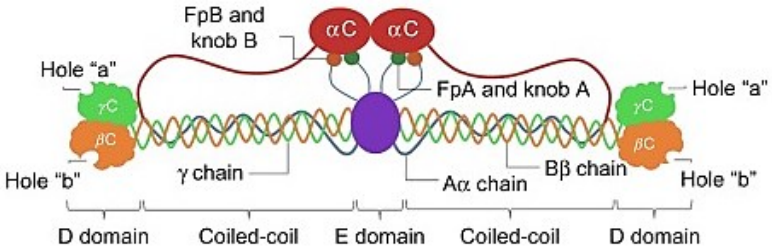


Figure 10 – Structure of fibrinogen molecule [37].

The polymerization of the fibrinogen molecule occurred by a thrombin-mediated cleavage of the N-terminal fibrin peptide and produces the fibrin protein. This process is initiated with thrombin, cleaving the fibrinopeptide A (FpA) of the Aα-chain in the N-terminal peptide sequence, exposing the knob A, resulting in an A:a binding. Subsequently, a double-stranded protofibril formation starts occurring, initiation the fibrin polymerization. Afterwards, fibrin peptide B (FpB)

is cleaved from the fibrinogen Bβ-chain exposing the knob B, resulting in a B:b binding. This leads a branching of fibrin protofibrils, which can occur in bilateral or in equilateral junctions. Once branching is complete a 3D network is formed, result in fibrin strands. However, the bounds in fibrin strands are inherently weak. The presence of factor XIII able the covalent cross-linking of fibrin strands, conferring stability and mechanical strength to the fibrin polymers. The polymerization process of fibrinogen into fibrin is shown in figure 11 [34, 36, 37].

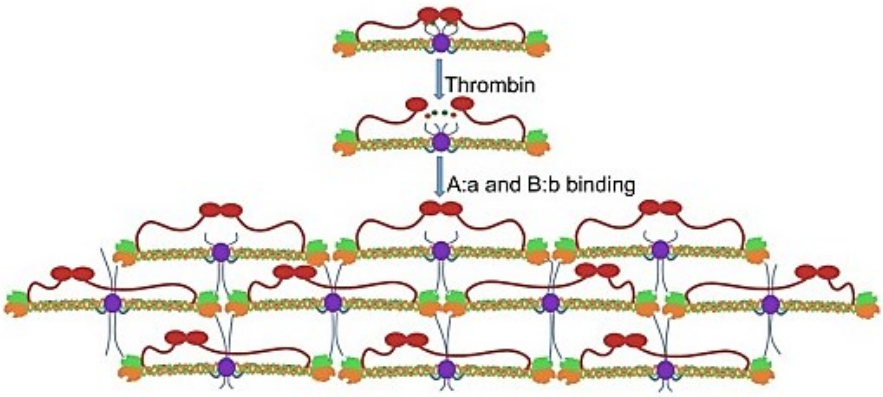


Figure 11 – Fibrin polymerization process, thrombin-mediated exposing the A and B knobs which leaves an A:a and B:b binding, forming the protofibrils, and subsequently their antiparallel cross-linking interaction result in a fibrin fibres [37].

The structure, stability, degradation properties, and mechanics of fibrin gels is directly linked to the thickness of the fibres, number of branch points, porosity, and permeability. Nevertheless, the polymerization conditions such as fibrinogen and thrombin concentrations, pH, Ca^{2+} concentration, and temperature affect the final characteristics of the fibrin gel. The final architecture of fibrin plays a critical role in cellular behaviour in the wound environment. The thrombin concentration directly affects the final characteristics of the fibrin formed. High concentration levels of thrombin result in thin fibres and thus leaves many branch points and small pore size geometry. Adversely, low concentration levels of thrombin results in thick fibres with low branch points and large pore size geometry [34, 36, 37].

2.3.4.2 Fibrin-based Hydrogel in Bone Tissue Engineering

Fibrin is a natural polymer, naturally present in the bone constitution, and it is critical in blood clotting and wound repair processes. In the bone tissue engineering field, fibrin-based hydrogels are a potential solution to treat injured tissues due to their homeostatic properties. In wound repair, fibrin minimizes blood loss, creates a barrier against microbial infection, and provides a degradable autologous scaffold important in cell activity during the repair of the defect. In addition to the haemostatic properties, fibrin performance an initial mechanical support for angiogenesis, and subsequently promoting cell infiltration and long-term tissue remodelling [37, 38]. For bone tissue engineering applications, fibrin-based hydrogels can be used as a cell delivery, delivery vehicle for antimicrobial agents, growth-factors delivery vehicle, or as injectable fibrin polymerized in *ex vivo* into scaffolds, thin layers, or films to treat defect problems. Usually, fibrin-based hydrogels are applied in the repair of adipose, cardiovascular, ocular, muscle, liver, skin, cartilage, and bone tissues [37].

2.3.4.3 Rheological properties of Fibrin Hydrogel

The 3D network of elongated cross-linked branches of fibrin strands confers viscoelasticity properties to the fibrin polymer. Thus, fibrin is a viscoelastic material, showing both elastic and viscous behaviours. The elastic property is characterized to current a reversible mechanical deformation, being described by shear storage modulus, G′. The viscous behaviour is characterized by showing an irreversible deformation (creep) under a stress force. This property is described by shear loss modulus, G″. Usually, the ratio G″/G′ describes the viscosity and stiffness of the final structure of fibrin. For a ratio G″/G′ > 1, the fibrin is more viscous than elastic. Subsequently, a ratio G″/G′ < 1 the fibrin response is more elastic than viscous. In addition to these rheological properties, fibrin exhibits a non-linear elasticity. Hence, the elastic modulus of fibrin at low strains is constant, and at larger strains strongly increases, as shown in figure 12. As the strain increase, the fibrin strands start to align in the strain direction, and the bend of the fibres becomes more difficult, increasing the stiffness of the polymer. This elastic characteristic of fibrin is named strain hardening or strain stiffening, being an advantageous property of fibrin gels. Biologically, this non-linear property allows the fibrin clot to be mechanically stiffer, supporting higher strains. Thus, their structural integrity is maintaining, preventing its embolization [38, 39].

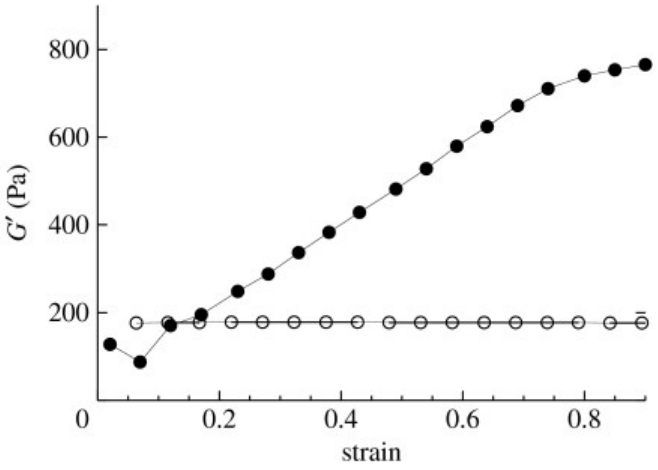


Figure 12 - Stress-strain curve of fibrin non-linear characteristic: (filled circles) 6 mg/ mL human fibrinogen polymerized under coarse clotting conditions, and (open circles) 5% polyacrylamide polymerized with ammonium persulphate and tetramethylethylenediamine (TEMED) [38].

2.3.4.3 Modification of mechanical properties of Fibrin

Fibrin mechanical properties and characteristics can be modified by different methods: fibrinogen and thrombin concentration; calcium additions; proteins incorporation; crosslinking agents (e.g., fibronectin or factor XIII). These strategies can modify fibrin thickness, network permeability, elastic modulus, and degradation properties, characteristics inherently related to the cell behaviour into the construct produced. The variation of overall fibrinogen and thrombin concentration is one of the simplest methods that can induce the modification of fibrin structure. Higher content of fibrinogen reduces the pore size geometry, leading to a less permeable matrix for oxygen and nutrients diffusion and cell infiltration. On the other hand, low thrombin concentration is associated with low gelation times, resulting in a thick fibres network with high porosity. Adversely, high levels of thrombin content result in highly branched thin fibrin networks

with low porosity. These characteristics lead to an increase in elastic modulus and ultimate tensile strength. Calcium additions can also affect fibrin network structure and mechanics. Increasing Calcium content in fibrin polymer leads to an increase in fibre size but a decrease in stiffness. Fibrin properties can also be modified by the addition of cells and fibrin-binding entities, or by the incorporation of proteins naturally present in the circulating of the blood (e.g., fibronectin) [36, 37].

Biologically, the increase of the stiffness of the fibrin gel has a direct impact on cell behaviour. Previous studies by *Bensaid et al*. showed that fibrin scaffolds with high levels of fibrinogen and thrombin result in a structure able to promote the spread, proliferation, and differentiation of cells. Adversely, a high concentration of fibrinogen and thrombin results in a denser structure affecting the normal cell behaviour. Another study done by *Catelas et al*. showed that fibrinogen concentration promotes a more open structure, increasing cell proliferation. Table 1 describe the effects of fibrinogen and thrombin concentrations changes in the mechanics and biological activity of the Fibrin hydrogel construct. These previous studies suggested that lower concentrations of fibrinogen promote an increase in cell proliferation, while a high concentration of fibrinogen promote an increase in cell differentiation. However, the higher content of fibrinogen leads to a decrease in final mechanical properties (e.g., compressive strength) [36, 37].

Table 1 - Structural/Biological Variables of variation of fibrinogen and thrombin concentrations (Adapted from [36])

Fibrinogen concentration	Thrombin concentration	Structural/Biological Variables	References
5 mg/mL	0.25–4 U/mL	The increase of thrombin concentration accelerates osteoblast differentiation.	[40]
10–80 mg/mL	5 U/mL	The increase of fibrinogen concentration leads a decrease one compressive strength and a decrease one final porosity. The cell adhesion and proliferation were promoted for high levels of fibrinogen.	[41]
5–50 mg/mL	2–250 U/mL	The variation of fibrinogen concentration expresses a higher affect in osteogenic differentiation under higher levels. The thrombin concentrations had a lesser effect.	[42]

Chapter 3

Materials and Methods

3.1 Materials

Type I collagen from Achilles's tendon bovine, phosphate buffered saline (PBS), Human Osteopontin (OPN), p-nitrophenol phosphate, trypsin EDTA, paraformaldehyde, sodium naphthyl phosphate, Fast Blue RR, sodium hydroxide (NaOH), Alizarin Red S, Ammonium hydroxide (NH_4OH), picric acid, and Picosirius red solution was purchased to Sigma-Aldrich (St. Louis, USA). Hydrochloric acid (HCl), 1-ethyl-3-(3-dimethyl aminopropyl) carbodiimide hydrochloride (EDC), and N-hydroxysuccinimide (NHS) was obtained from Merck (Germany). Nanohydroxyapatite aggregates (nanoHA) were provided from Fluidinova S.A (Maia, Portugal). Tris-phosphate buffered saline (TBS) was prepared in lab by mixing 134 mM sodium chloride (NaCl), 2.7 mM KCl (Potassium chloride) and 33 mM tris(hydroxymethyl)aminomethane (TRIS), all reagents were purchased to Sigma-Aldrich (St. Louis, USA). Culture cell medium Dulbecco's Modified Eagle Medium was purchased to DMEM – HyClone.

3.2 Preparation of Collagen/nanohydroxyapatite Scaffolds

Coll/nanoHA scaffolds were prepared from the cryogelation technique. Firstly, type I insoluble collagen was swelled overnight in 10 mM chloride acid (HCl) solution at 4°C at a concentration of 2 % (w/v). The dispersion was then homogenized (Ultra Turrax T25, IKA) at 11000 rpm for 2 hours and centrifuged at 2000 gf for 5 minutes. Coll/nanoHA composite cryogel was prepared with 5 ml of collagen slurry diluted in 4.5 mL of HA (nanometric) suspended in 10 mM chloride acid (HCl). The dry powders of HA (nanoparticles) were mixed with the chloride acid solution in a particular ratio and vortex to homogenize (final composition Coll/nanoHA 50:50). To the preparation of cryogels, 20 mM NHS and 40 mM EDC were added to the collagen slurry and immediately transferred to a syringe (2 ml) that was used as a mould. Finally, the scaffold was thawed at room temperature. Subsequently, the samples were washed with distilled water. The samples were frozen overnight and dried with a freeze-dryer (Labconco, FreeZone 6) at a vacuum oven at -80ºC and 0.1 bar for 24 h. The Coll/nanoHA samples were cut with 4 mm width.

3.3 Fibrin-OPN Hydrogel

3.3.1 Preparation of Fibrin Hydrogel

Fibrinogen solution (Fb) was prepared dissolving in Tris-buffered saline (TBS, pH 7.4) to 20 mg/ml. Fibrin gels (total volume 100 µl) were obtained by mixing equal volumes of the fibrinogen

solution and a thrombin solution (Tb) in TBS containing $CaCl_2$ [final concentration of 1, 2, and 3.5 National Institute of Health (NIH) U/ml thrombin from human plasma; 2.5 mM $CaCl_2$; prepared for a final volume of 250 µL. Four different fibrin hydrogels were produced: Fb LTb 1:1 (10 mg/ml and 1 NHI U/mL); Fb HTb 1:1 (10 mg/ml and 3.5 NHI U/mL); Fb LTb 1:2 (6.3 mg/ml and 1 NHI U/mL); Fb HTb 1:2 (6.3 mg/ml and 2 NHI U/mL). For the homogenizing of the final solution, the thrombin working solution was gently pipetting up and down with fibrinogen. Immediately, the fibrin gel crosslinking was induced in a 37ºC incubated with a CO_2 atmosphere for 30 minutes. Finally, was added PBS solution to the fibrin hydrogels.

3.3.2 Preparation of OPN

Human Osteopontin (OPN) solutions were prepared by dilution in tris-phosphate buffered saline (TBS) with pH of 7.4, at concentrations of 10 and 100 µg/mL, low concentration (LC), and high concentration (HC) OPN solution, respectively.

3.3.3 Preparation of Fibrin - OPN Hydrogel

The OPN solution (10 µL) was initially mixed with a fibrinogen solution (20 mg/mL) and then added to the thrombin/$CaCl_2$ solutions (final concentrations: 6.3 mg/mL of Fb, 2 NHI U/mL of Tb and 2.5 mM of $CaCl_2$) with a final volume of 100 µl. Subsequently, the gelation process was finished at 37ºC for 30 minutes.

3.4 Preparation Coll/nanoHA - Fibrin Hydrogel composite

The Coll/nanoHA cryogel scaffolds produced were soaked with the following 4 different fibrin gel solutions described before (3.3.1). Coll/nanoHA – Fibrin Hydrogels with and without OPN (High and Low concentration) were produced.

3.5 Rheological Characterization of Coll/nanoHA Scaffold - Fibrin Hydrogel

3.5.1 Dynamic Mechanical Analysis

Biomechanical properties of the different proportions of fibrin gel within Coll/nanoHA scaffolds with or without OPN (LC and HC) were analysed by Tritec2000 dynamic mechanical analyser (Triton Technology, UK). This technique, by applying an oscillatory force to a sample, allows evaluating its mechanical response. Thus, is possible to analyse viscosity and elasticity to the material, from the phase lag and the stiffness (modulus) recovery of the sample. The subjected tests to samples were cycles of compression with frequencies varying between 0.1 Hz and 15 Hz at 37ºC. The sample's diameter was previously measured by a Vernier calliper tool and incubated at 37ºC before testing. Three samples of each different biocomposite were analysed. The results (Storage Modulus, Loss Modulus, Tan Delta) were showed as average value.

3.5.2 Viscoelasticity Analysis

The viscoelasticity of the fibrin hydrogel samples and Fb 1:2 HTb/ OPN (LC and HC) were analysed by a Kinexus Pro rheometer (Malvern). The fibrin hydrogel samples were punched from the original ones with a cylinder diameter of 4 mm and incubated at 37ºC before testing. All measurements were performed at 37ºC using a plate-and-plate geometry with 4 mm diameter. The samples were compressed in 30% of their original thickness to avoid slippage. Initially, a stress sweeps test was performed with a 0.1 Hz frequency to evaluate the linear viscoelastic region (LVR) of the samples. Frequency sweeps between 0.01–2 Hz were then performed within the LVR. Three samples of each fibrin hydrogel combination were analysed. The average tan delta, Storage modulus (G'), and Loss modulus (G'') were calculated.

3.5.3 Statistical Analysis

Data were presented as mean and standard deviation, and they were analysed using the two-way ANOVA test (GraphPAD software). Differences between groups were considered statistically significant when $p < 0.05$.

3.6 *In vitro* biological studies

3.6.1 Cell Culture

Human osteoblast-like cells (MG63; ATCC) were cultured in Dulbecco's Modified Eagle Medium supplemented with 10% fetal bovine serum (Gibco), 1% penicillin-streptomycin ($3x10^4$ mol/L and $5x10^4$ mol/L; Gibco) and maintained at 37ºC and 5% of carbon dioxide (CO_2). After cell confluence of 90% on T flask (75 cm^2; Nunc), cells were washed with PBS solution, detached with trypsin solution (0.5%) at 37ºC for 5 min, and counted using a Neubauer chamber. Cells were seeded on 48 well-plate (Nunc, $5x10^4$ cells/well). The culture medium was changed every 3 days. The evaluated time points were 1, 3, 6 days. At the same time, Coll/nanoHA/Fb scaffolds with or without OPN (LC and HC) were incubated into a complete medium for 24 h (1g of material/10 ml of complete medium). The degradation products of Coll/nanoHA/Fb scaffolds with or without OPN (LC and HC), was then diluted with different percentages in a culture medium: 100% (only composite medium), 50% (composite medium/culture medium in a relationship of 1:1), and 25% (composite medium/culture medium in a relationship of 1:3).

3.6.2 Metabolic Activity

Cell vitality was assessed with the nontoxic Alamar blue dye (resazurin) test. Resazurin is reduced by intracellular enzyme activity to resofin, a fluorescent form of Alamar Blue. Work solution of 10% (vol/vol) fluorescent dye was diluted to 2% and added to the well-plate (300 µl) and incubated at 37ºC for 2 h in a humidified atmosphere of 95% air and 5% CO_2 for 4 h. The solution was then transferred into a black 96-well plate, and fluorescence intensity was measured by a plate reader (Synergy; BioTek) at 530 and 590 nm for excitation and emission, respectively.

3.6.3 Alkaline Phosphatase Activity

The alkaline phosphatase activity (ALP) was measured as quantitative analysis for early osteogenic characterization. To perform this assay, the ALP enzyme activity was followed through

substrate hydrolysis, using p-nitrophenol phosphate at pH 10. After incubation at 37ºC, the reaction was stopped by adding NaOH (0.02 M) and p-nitrophenol was quantified at 405 nm, using a plate reader (Synergy MX, BioTek). Finally, the ALP results were expressed in nanomoles (nmol) of p-nitrophenol produced per minute (min).

3.6.4 Histocytochemical Staining

Histocytochemical staining was performed after 6 days of cell culture, described in section 3.6.1. Phosphate deposits were assessed by the von Kossa assay. The cultures were covered with a 1.0 % silver nitrate solution and kept for 1 h under UV light. After the samples had been washed with distilled water, a 5.0 % sodium thiosulfate solution was added for 2 min and cultures were washed again. Phosphate deposits were stained brown. For Collagen Type I staining, 1% picric acid solution and picosirius red solution were used. Cells were covered by picosirius red solution for 1 hour and washed with HCl solution (10mM). Type I collagen was stained in red. After drying, the cells were evaluated by Inverted Optical microscopy (Axiovert 200M, Zeiss).

3.6.5 Statistical Analysis

Data were presented as mean and standard deviation, and they were analysed using the two-way ANOVA test (GraphPAD software). Differences between groups were considered statistically significant when $p < 0.05$.

Chapter 4

Results

4.1 Rheological characterization of Coll/nanoHA Scaffold-Fibrin Hydrogel

4.2.1 Dynamic Mechanical Analysis

The Dynamic Mechanical Analysis (DMA) assay was performed to evaluate the mechanical response of Coll/nanoHA scaffolds with Fb hydrogels incorporations, with or without the presence of OPN protein at high and low concentrations.

4.2.1.1 Coll/nanoHA scaffolds – Fibrin Hydrogels

The variations of storage modulus (E') with the increase of frequency for the Coll/nanoHA scaffolds and Coll/nanoHA scaffolds with Fibrin hydrogels (different thrombin and fibrinogen proportions) are showed in figure 13. As it is possible to see in the figure, the higher E' modulus is observed for the composite Coll/nanoHA_Fb 1:2 HTb with a final concentration in the fibrin hydrogel of 6.3 mg/mL of fibrinogen and 2 NHI (U/mL) of thrombin. The composite material Coll/nanoHA_Fb 1:1 LTb howed the lower E' modulus values. The Coll/nanoHA scaffold was the material with the lowest E' modulus when compared to the scaffolds with the fibrin hydrogel incorporations. Hence, the elastic properties of the Coll/nanoHA scaffold were enhanced by fibrin hydrogel incorporations. Results of the DMA assay shown that the increase of thrombin concentration provided a higher E' modulus and the increase of fibrinogen concentration led to a decrease in the final E' modulus.

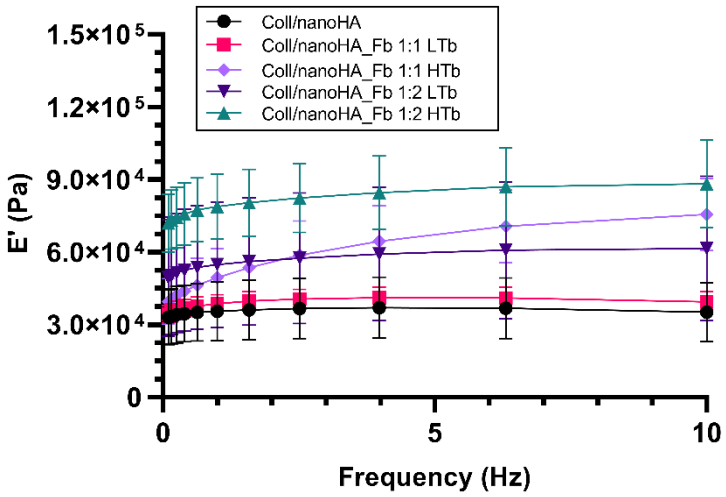


Figure 13 - Storage modulus (E') of the Coll/nanoHA/Fb samples under dynamic compression solicitation versus frequency (0.1 Hz to 10 Hz).

Figure 14 shows the E' modulus to the frequency values of 0.1 Hz and 10 Hz, separately. These results highlight a higher tendency of the increase in E' modulus with the increase of thrombin concentration in the fibrin hydrogel. Therefore, the composite biomaterials with a higher Tb proportion shown a higher E' modulus. For a frequency value of 0.1, all the samples showed a lower E' modulus, when compared to the 10 Hz frequency. On the sample Coll/nanoHA_Fb 1:2 HTb, it was observed an increased tendency of final E' modulus with higher frequency values, increasing from $7.2x10^4 \pm 1.2x10^4$ Pa to $8.8x10^4 \pm 1.8x10^4$ Pa.

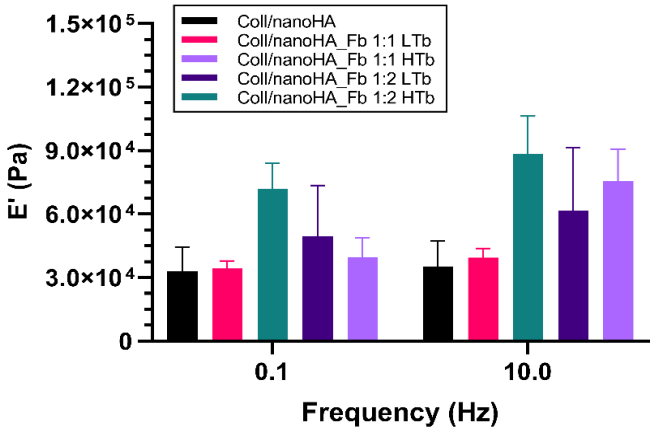


Figure 14 - Storage modulus (E') of the Coll/nanoHA/Fb samples under compression solicitation with frequency of 0.1 and 10 Hz.

The loss modulus (E'') variation with the increase of frequency for Coll/nanoHA scaffolds and Coll/nanoHA scaffold with Fibrin hydrogels incorporations is shown in figure 15. Results showed a marked increase of E'' modulus for all the samples with the increase of frequency. The composite with higher content of Tb showed a higher increase (Coll/nanoHA_Fb 1:1 HTb and Coll/nanoHA_Fb 1:2 HTb). Figure 16 shows the specific E'' modulus to the frequency of 0.1 Hz and 10 Hz for all the samples. It was possible to observe that the samples Coll/nanoHA_Fb 1:1 HTb and Coll/nanoHA_Fb 1:2 HTb shown the highest E'' modulus for both frequencies of 0.1 and 10 Hz. Moreover, could be observed a significant increase in the E'' modulus with the increase of frequency. For the Coll/nanoHA_Fb 1:2 HTb sample, the E'' modulus increase from $9.3x10^3 \pm 1.5x10^3$ Pa to $3.4x10^4 \pm 1.5x10^4$ Pa.

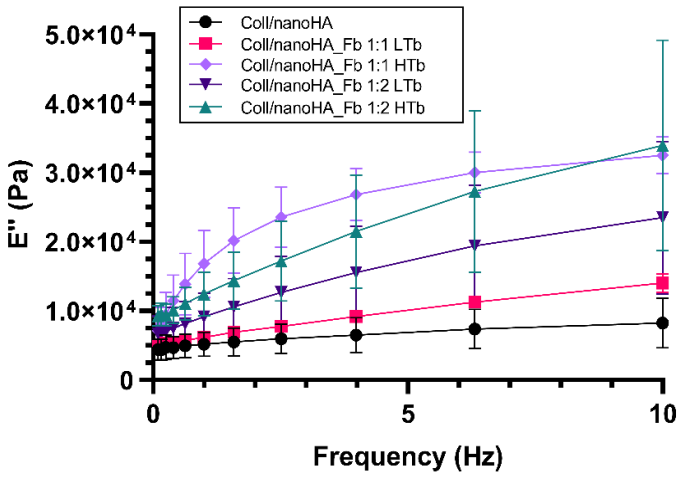


Figure 15 - Loss modulus (E'') of the Coll/nanoHA/Fb samples under dynamic compression solicitation versus frequency (0.1 Hz to 10 Hz).

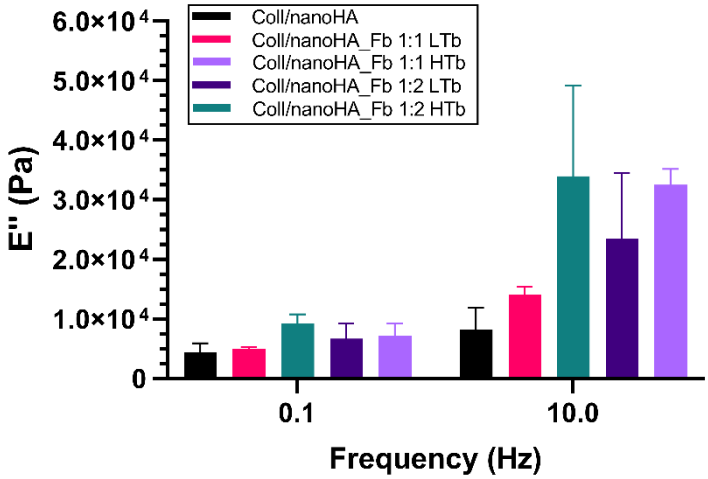


Figure 16 - Loss modulus (E'') of the Coll/nanoHA/Fb samples under compression solicitation with frequency of 0.1 and 10 Hz.

The loss factor (tan delta) is described by the ratio between the loss modulus (E'') and storage modulus (E'), providing information about the viscoelastic behaviour of the material. The higher the tan δ value, the higher the E'' component of the material and lower the E'. Figure 17 shows the tan δ of the samples with the increase of frequency. As observed in the graph, all the samples showed a tendency to become more viscous than elastic with the increase in frequency. At the lowest values of frequency, the composite is more elastic, with a higher capacity for storing energy. Nevertheless, at high frequencies, they become more viscous and tougher. The samples Coll/nanoHA_Fb 1:1 HTb and Coll/nanoHA_Fb 1:2 HTb demonstrate a more viscous behaviour than elastic with the increases of frequency. The incorporation of fibrin hydrogels with a Coll/nanoHA scaffold resulted in an improvement in the viscosity of the scaffold without losing the capacity of storing energy.

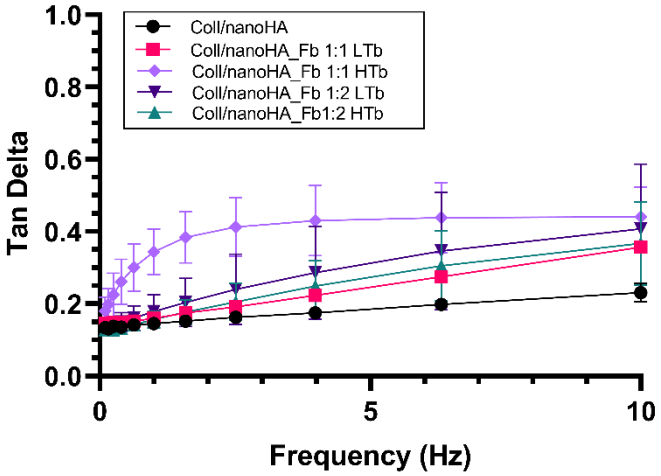


Figure 17 - Tan δ of the samples under dynamic compression solicitation versus frequency (0.1 Hz to 10 Hz).

4.2.1.2 Coll/nanoHA scaffolds - Fibrin Hydrogels- OPN

DMA analyses were performed to better understand the mechanical influence of OPN protein in the scaffolds with fibrin hydrogels incorporations. In this test, the Coll/nanoHA_Fibrin 1:2 HTb composite was only considered, due to the higher rheological properties demonstrated previously, comparatively to the other composite materials. The Coll/nanoHA_Fibrin 1:2 HTb sample were studied for different OPN concentrations (10 and 100 µg/mL). Figure 18 shows the storage modulus (E') with the increase of frequency for the samples with low OPN concentration (LC) and high concentration (HC). As it could be seen in the graph, the incorporation of OPN protein increases the viscoelastic properties of the Coll/nanoHA_Fb 1:2 HTb composite with a high OPN concentration (100 µg/mL). For the composite with lower OPN concentration (10 µg/mL), the rise of E' modulus with the frequency is lower when compared to the Coll/nanoHA_Fb 1:2 HTb composite (only Fibrin hydrogel).

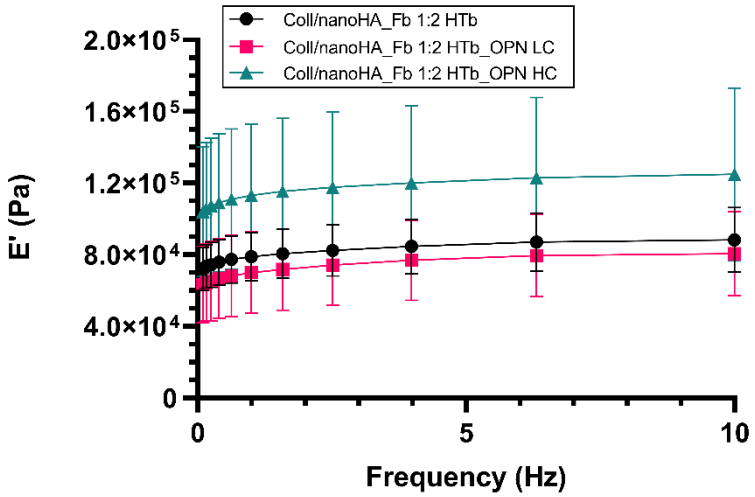


Figure 18 - Storage modulus (E') of the Coll/nanoHA_Fb 1:2 HTb samples with Low concentration (LC) and High concentration (HC), under dynamic compression solicitation versus frequency (0.1 Hz to 10 Hz).

Figure 19 shows the E' modulus to 0.1 Hz and 1 Hz frequencies for all different samples analysed. For a frequency of 0.1 Hz, all samples showed lower E' modulus, when compared to high-frequency values (10 Hz). The Coll/nanoHA_Fb 1:2 HTb_OPN HC sample highlights the higher E' modulus for both frequency values (0.1 and 10 Hz). Nevertheless, the Coll/nanoHA_Fb 1:2 HTb and Coll/nanoHA_Fb 1:2 HTb_OPN LC composites shown the lowest E' modulus. However, the lower OPN concentration showed a tendency of an increase of the E' modulus under compression at lower and higher frequency values (0.1 and 10 Hz).

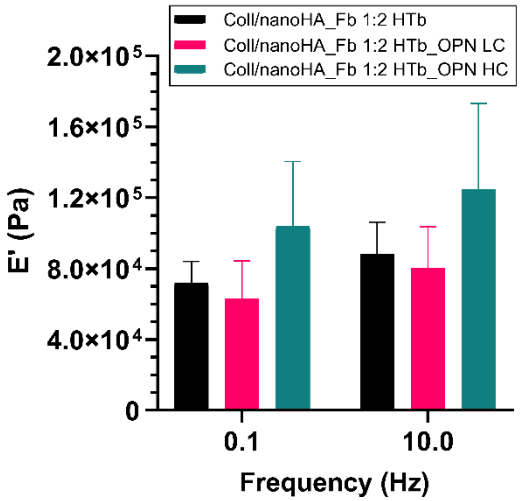


Figure 19 - Storage modulus (E') of the Coll/nanoHA_Fb 1:2 HTb samples with OPN Low concentration (LC) and High concentration (HC), under compression solicitation with frequency of 0.1 and 10 Hz.

Figure 20 shows the loss modulus (E") to the samples Coll/nanoHA_Fb 1:2 HTb with OPN LC and HC. As it is possible to observe, the increase of the frequency provided a marked increase in the E'' modulus, for all the samples in the study. The Coll/nanoHA_Fb 1:2 HTb_OPN HC showed the highest E'' modulus, followed by the Coll/nanoHA_Fb 1:2 HTb sample. Therefore, the OPN at the highest concentration led to an increase in mechanical properties of the Coll/nanoHA_Fb 1:2 HTb. In contrast, the lower OPN concentration provided a decrease of the E" (lower stiffness). Figure 21 shows the E" modulus of the samples to the 0.1 Hz and 10 Hz frequencies. In concordance with the previous graph (Fig.20), is possible to observe the higher E'' modulus for the highest frequency (10 Hz). Nevertheless, for an OPN concentration of 10 µg/mL (LC) is observed a less noticeable increase in E" modulus. The Coll/nanoHA_Fb 1:2 HTb_OPN HC (100 µg/mL) sample shows a similar behaviour comparatively with Coll/nanoHA/Fb 1:2 HTb sample, with an E'' modulus at 10 Hz frequencies of $2.3x10^4 \pm 1.5x10^4$ Pa and $3.4x10^4 \pm 1.5x10^4$ Pa, respectively.

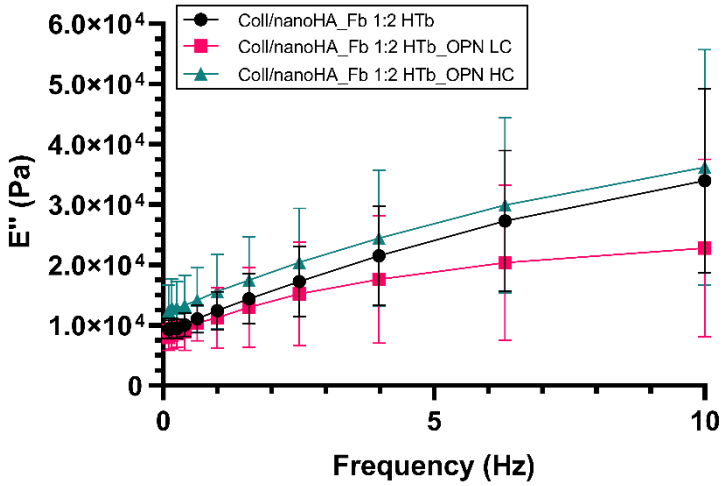


Figure 20 - Loss modulus (E'') of the Coll/nanoHA_Fb 1:2 HTb samples with OPN Low concentration (LC) and High concentration (HC), under dynamic compression solicitation versus frequency (0.1 Hz to 10 Hz).

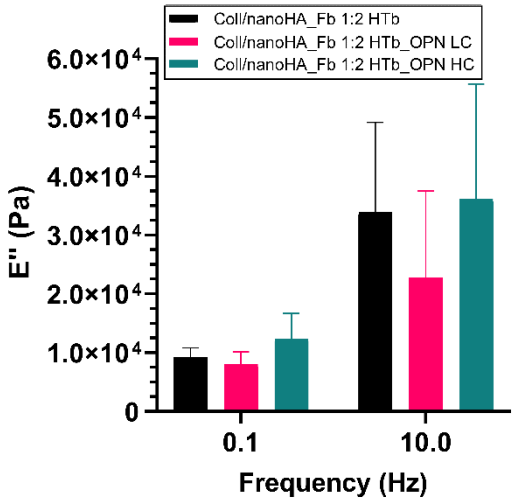


Figure 21 – Loss modulus (E'') of the Coll/nanoHA_Fb 1:2 HTb samples with OPN Low concentration (LC) and High concentration (HC), under compression solicitation with frequency of 0.1 and 10 Hz.

The loss factor (tan δ), the ratio between E'' and E' modulus, is shown in the graph in figure 22 for the Coll/nanoHA/ Fb 1:2 HTb samples with OPN LC and HC. Results showed a tendency for all composites to become more viscous and less elastic with the increase of frequency. Although, the Coll/nanoHA_Fb 1:2 HTb_OPN HC evidence the lowest tan δ for all frequencies. Therefore, the OPN protein incorporation in Coll/nanoHA/Fb composite does not provide significant mechanical properties influence, especially at high concentrations.

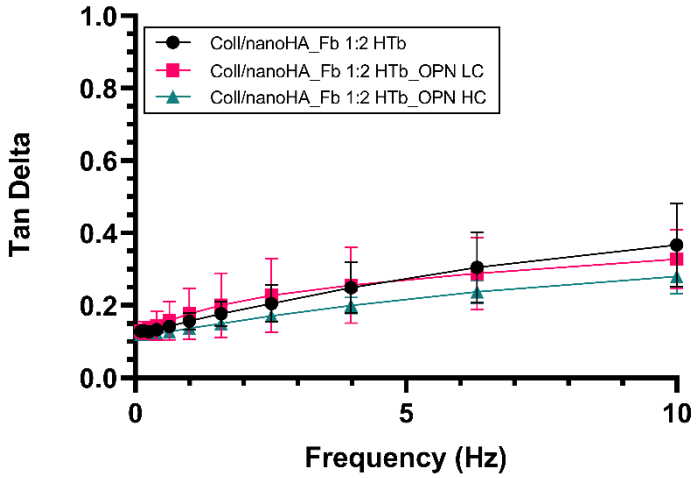


Figure 22 - Tan δ of the Coll/nanoHA_Fb 1:2 HTb samples with OPN Low concentration (LC) and High concentration (HC), under dynamic compression solicitation versus frequency (0.1 Hz to 10 Hz).

4.2.2 Viscoelasticity Analysis

Rheometer technique was applied to the characterization of fibrin hydrogels with different compositions of thrombin and fibrinogen. The OPN influence on the mechanical behaviour of the hydrogels was also studied. The statistical test two-way ANOVA was performed for the different samples at 0.1 Hz frequency and 1 Hz frequency.

4.2.1.1 Fibrin Hydrogels

Storage modulus (G') analysis (Figure 23) showed that there was a similar behaviour of different Fibrin hydrogels, under shear stress forces with an increase in frequency (0.01-2 Hz) by G' modulus calculation. The increase of frequency at approximately 1.5 Hz shows an increase in G' modulus, decreasing from this point until 2 Hz of frequency. For higher frequencies (above 1.0 Hz) the Fb 1:1 LTb shows the higher G' modulus. Subsequently, to the Fb 1:1 HTb sample is observed the lowest G' modulus.

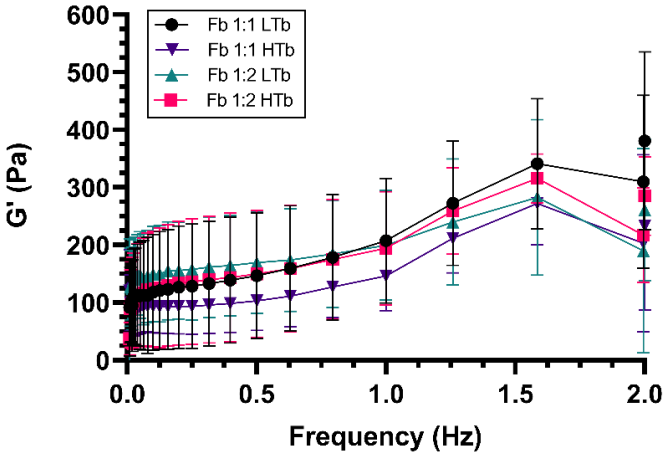


Figure 23 - Storage modulus (G') of the Fb hydrogels samples under a shear stress force versus frequency (0.01 Hz to 2 Hz).

Figure 24 shows G' modulus at compression with low frequency (0.1 Hz) and high frequency (1 Hz), for the different samples in study. Results showed there was a marked increase of G' modulus to the Fb 1:1 Ltb hydrogel from 0.1 Hz to 1 Hz frequency. It was possible to observe that the lowest Tb concentration (with equal Fb concentration in the hydrogel) led to a tendency in the increase of G' modulus. Therefore, a two-way ANOVA statistical test was performed for these two different frequency values, and no statistical difference was observed.

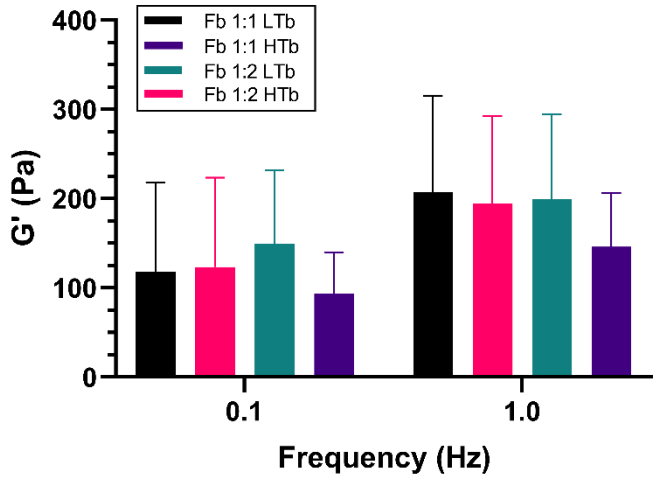


Figure 24 - Storage modulus (G') of the Fb hydrogels samples under a shear stress force to frequency values of 0.1 Hz and 1 Hz).

Figure 25 represents the viscoelastic behaviour of the Fibrin hydrogels. As it could be observed, the increase of frequency led to an increase in shear loss modulus (G'') of the fibrin samples, with a marked influence above 1 Hz frequency. All the Fibrin hydrogels samples show similar behaviour of the increase of the G'' modulus with the frequency. Therefore, Fb 1:2 HTb hydrogel sample showed the highest G'' modulus, until 2 Hz of frequency. In contrast to the graph of G' modulus (Fig. 23), Fb 1:1 LTb sample shows the lowest G'' modulus.

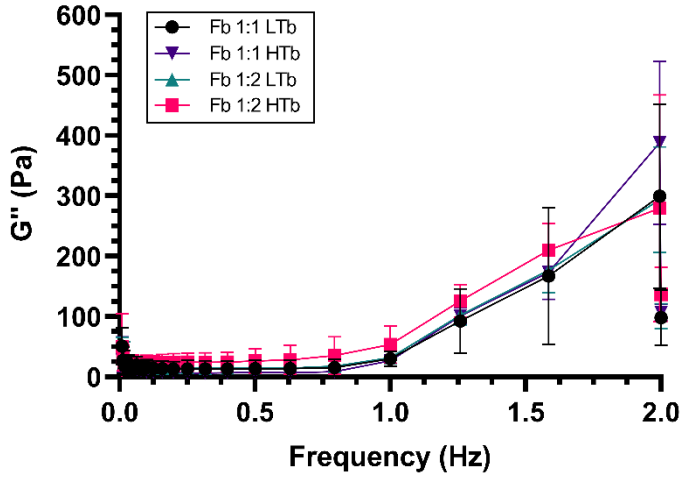


Figure 25 - Loss modulus (G'') of the Fb hydrogels samples under a shear stress force versus frequency (0.01 Hz to 2 Hz).

Figure 26 shows the G'' modulus to 0.1 Hz and 1 Hz frequency to the hydrogel's samples. The Fb 1:2 HTb shows the highest G'' modulus for the frequency of 0.1 Hz and 1 Hz, increasing from 23 ± 28 Pa to 53± 66 Pa, respectively. The two-way ANOVA test was performed for the different hydrogel samples under shear stress forces at 0.1 Hz and 1 Hz, and no statistical difference was observed.

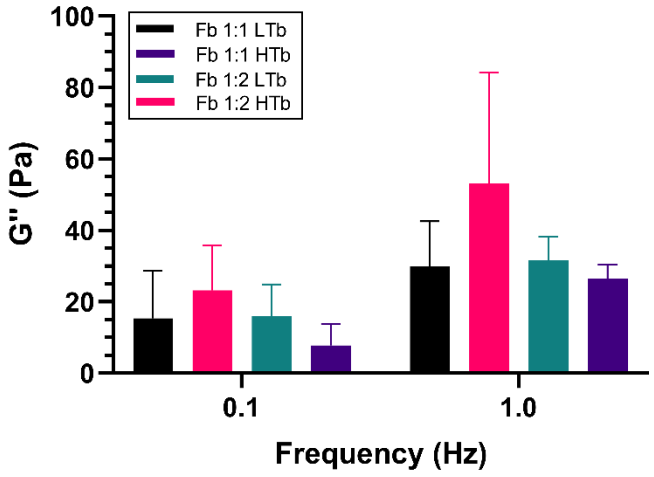


Figure 26 - Loss modulus (G'') of the Fb hydrogels samples under a shear stress force to frequency values of 0.1 Hz and 1 Hz).

Figure 27 shows the variation of loss factor (tan δ) with the frequency. For all the fibrin hydrogels, the tan δ increased with the enhancement of the frequency indicating that the samples become more viscous and less elastic. The Fb 1:2 LTb samples are showed the highest tan δ values, followed by Fb 1:1 HTb sample. The Fb 1:1 LTb shows the lowest loss factor. Therefore, the increase of thrombin concentration (maintaining the Fb content) increases the loss factor of the hydrogel. This enhancement in the mechanic strength of the gel occurs without the total loss of elasticity of the composite.

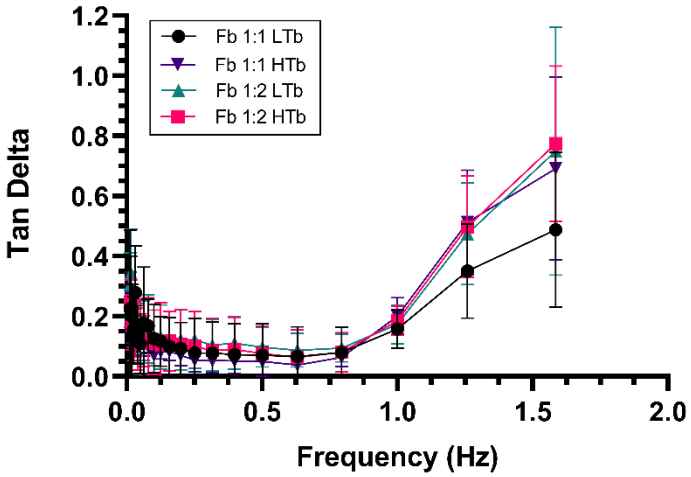


Figure 27 - Tan δ of the samples under shear stress force versus frequency.

4.2.1.2 Fibrin - OPN Hydrogels

Rheological assay was performed to evaluate the influence of OPN protein on the rheological properties of the fibrin hydrogels. Since the Fb 1:2 HTb sample showed the highest rheological properties, these Fb and Tb concentrations were used to be modified by OPN with high and low concentrations. Figure 28 shows the variation of the shear storage modulus (G') with the respect to the frequency. As it may be seen, the Fb 1:2 HTb sample highlights a higher G' modulus, when compared to the fibrin hydrogels with OPN protein incorporations at high concentration (100 µg/mL) and low concentration (10 µg/mL). Therefore, the OPN protein does not promote an increase in the elastic component of the fibrin hydrogel, especially at the lowest concentrations.

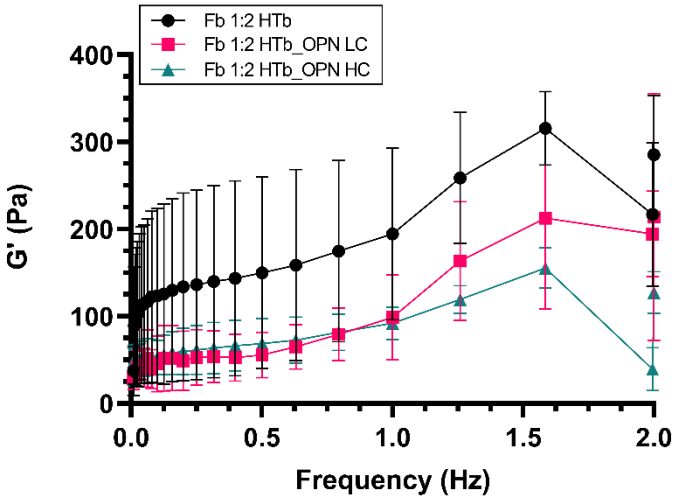


Figure 28 - Storage modulus (G') of the Fb hydrogels with OPN Low concentration (LC) and High concentration (HC) samples under a shear stress force versus frequency (0.01 Hz to 2 Hz).

For the frequencies of 0.1 Hz and 1 Hz, the G' modulus is shown in figure 29. It was possible to observe an increase in G' modulus of the hydrogel samples from the frequency of 0.1 Hz to 1 Hz. Fb 1:2 HTb sample shows the higher G' modulus for both frequencies. The two-way ANOVA statistical test was performed, and no statistical difference was observed.

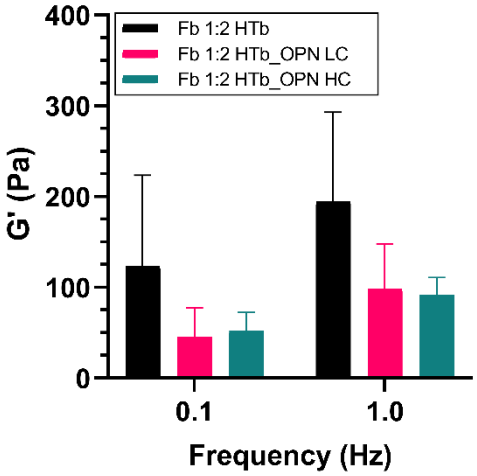


Figure 29 - Storage modulus (G') of the Fb hydrogels with OPN Low concentration (LC) and High concentration (HC) samples under a shear stress force to frequency values of 0.1 Hz and 1 Hz.

The shear loss modulus (G'') with the respect frequency (Fig. 30) of the samples with OPN LC and HC shows an improvement in the viscous component of the hydrogel with the OPN incorporation, above 1.5 Hz frequencies. With these results it also possible to observed that the high OPN concentration tended to decrease the G'' modulus of the hydrogel.

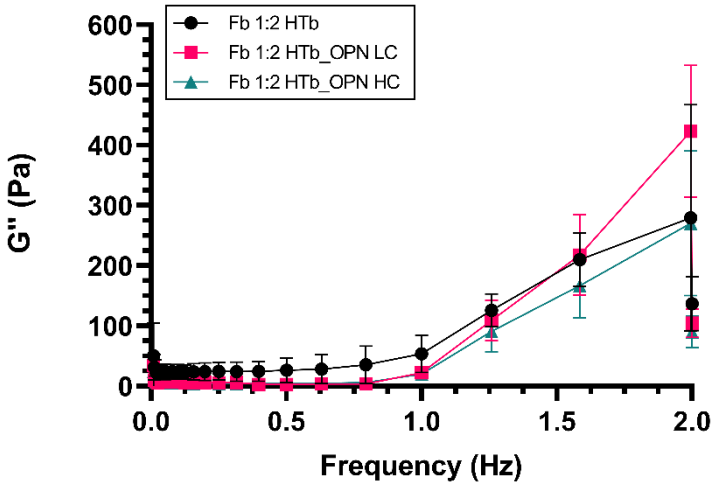


Figure 30 - Loss modulus (G'') of the Fb hydrogels with OPN Low concentration (LC) and High concentration (HC) samples under a shear stress force versus frequency (0.01 Hz to 2 Hz).

The G'' modulus for the frequencies of 0.1 Hz and 1 Hz (Fig. 31) shows a highlighted shear modulus to the Fb 1:2 HTb hydrogel sample. As it could be observed, the OPN incorporation at high and lowest concentrations provides a decrease the G'' modulus of the hydrogel, for both frequencies. The two different concentrations of OPN show a similar G'' modulus at 0.1 and 10 frequencies. The two-way ANOVA statistical test was performed between the two different frequency values and no statistical difference was observed.

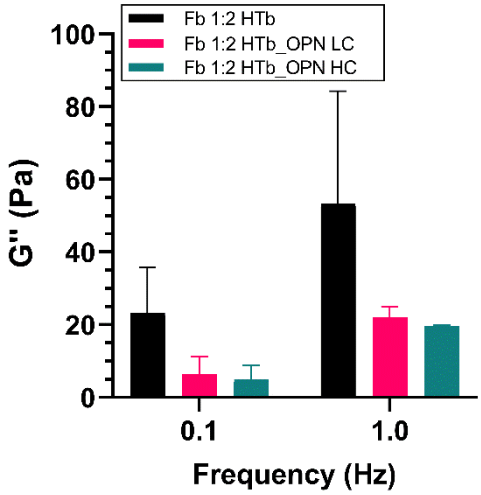


Figure 31 - Loss modulus (G'') of the Fb hydrogels with OPN Low concentration (LC) and High concentration (HC) samples under a shear stress force to frequency values of 0.1 Hz and 1 Hz).

The loss factor (Fig.32) for the samples whit OPN Low concentration (LC) and High concentration (HC) indicate a more viscous behaviour of the hydrogel with the incorporation of OPN protein when compared to the fibrin-only sample. This behaviour is more evident at high frequency (1 Hz). At the lowest frequencies, the samples showed a more elastic behaviour. The Fb 1:2 HTb without OPN tend to enhance the loss factor for the lowest frequencies.

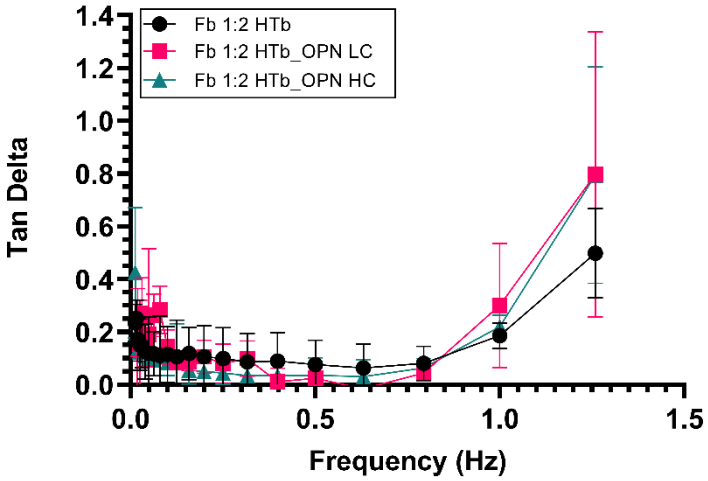


Figure 32 - Tan δ of the samples under shear stress force versus frequency.

4.3 *In vitro* Biological Studies

The metabolic activity, ECM composition, and differentiation of the human osteoblast-like cells (MG63) cultured with elution's of different scaffold/Fibrin composite with low and high OPN concentration (materials' degradable products medium and respective dilutions – 50% and 25% in completed cellular medium) was evaluated at 3 time-points (day 1, 3, and 6).

4.3.1 Metabolic Activity

Figure 33 shows the metabolic activity of the MG63 cultured with Coll/nanoHA_Fb 1:2 HTb composite elution's after 1, 3, and 6 days. The Alamar blue values of the cells cultured were similar in all samples, between 80-90% (control without materials degradation products was considered 100%) at different time-points. Is it possible to observe, the composite Coll/nanoHA_Fb 1:2 HTb indicates no evidence of cytotoxicity behaviour, presenting higher MG63 cell viability and proliferation rate. The two-way ANOVA test statistical analysis was performed for all the samples. The resazurin values of cells cultured Fb 100 and Fb 25 between day 3 and 6, and Fb 100 and Fb 50 on day 3 shown significant statistical differences.

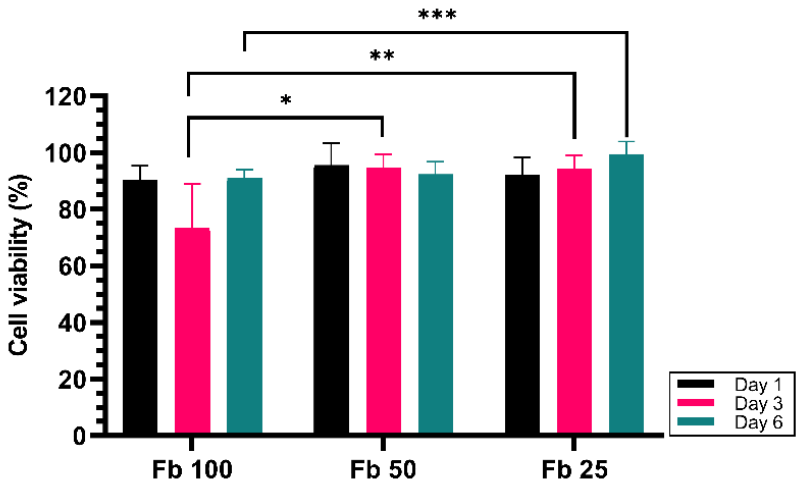


Figure 33 - Metabolic activity of MG63 cells after culture on Coll/nanoHA_Fb 1:2 HTb sample with different elution's (only-substrate medium, 1:1 and 1:3, respectively) for 1, 3 and 6 days, estimated by Resazurin assay. The control, culture (TCPS) was considered 100% (*, significantly different comparing Fb 100 (only-substrate medium) with Fb 50 (1:1 substrate medium /cell culture medium) on the same time point (day 3), $p<0.005$); (**, significantly different comparing Fb 100 (only-substrate medium) with Fb 25 (1:3 substrate medium /cell culture medium) on the same time point (day 3), $p<0.006$); (***, significantly different comparing Fb 100 (only-substrate medium) with Fb 25 (1:3 substrate medium /cell culture medium) on the same time point (day 6), $p<0.02$).

Resazurin assay was used to evaluate the metabolic activity of the MG63 cells (Fig.34) with the Coll/nanoHA scaffold_Fb 1:2 HTb_OPN LC (10 µg/mL) composite. All the results of the resazurin assay indicated an increase on cell proliferation at day 3, decreasing on day 6. The OPN LC 50 and OPN LC 25 samples showed a significant statistical difference. Nevertheless, with these results was possible to observe an increase in cell viability and proliferation with the incorporation of OPN protein in the biocomposite when compared with the previous results (Fig.33).

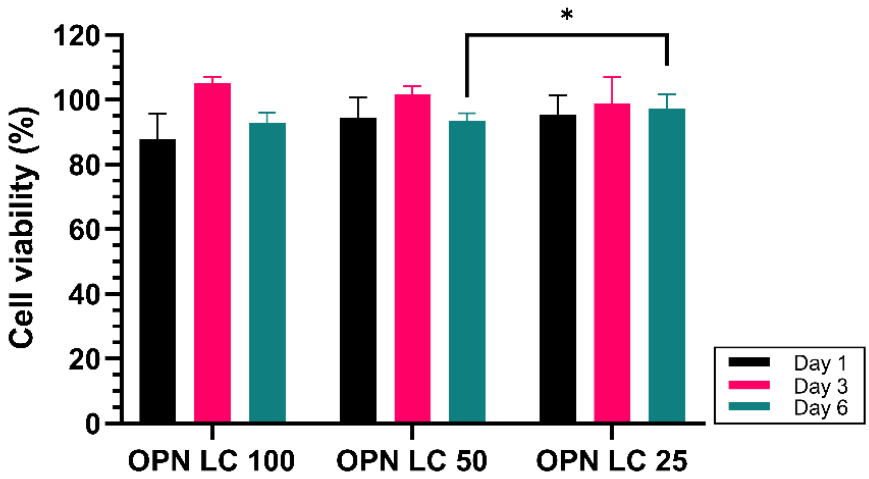


Figure 34 - Metabolic activity of MG63 cells after culture on Coll/nanoHA_Fb1:2 HTb_OPN LC (10 µg/mL) sample with different elution's (only-substrate medium, 1:1 and 1:3, respectively) for 1, 3 and 6 days, estimated by Resazurin assay. the control, culture (TCPS) was considered 100% (*, significantly different comparing OPN LC 50 (1:1 substrate medium/cell culture medium) with OPN LC 25 (1:3 substrate medium /cell culture medium) on the same time point (day 6), $p<0.037$).

Finally, the metabolic activity of the MG63 cells with the Coll/nanoHA scaffold_Fb 1:2 HTb_OPN HC (100 µg/mL) composite (Fig.35) shows an increase in cell proliferation activity between days 1, 3, and 6, with higher cell metabolic activity at day 6. Statistical differences were observed between OPN HC 100 and OPN HC 25 at day 1, OPN HC 100 and OPN HC 25 and day 3, and OPN HC 100 and OPN HC 50 at day 6. Therefore, the OPN protein at the highest concentrations led to an increase in cell proliferation, when compared with the lowest OPN concentrations (Fig.34).

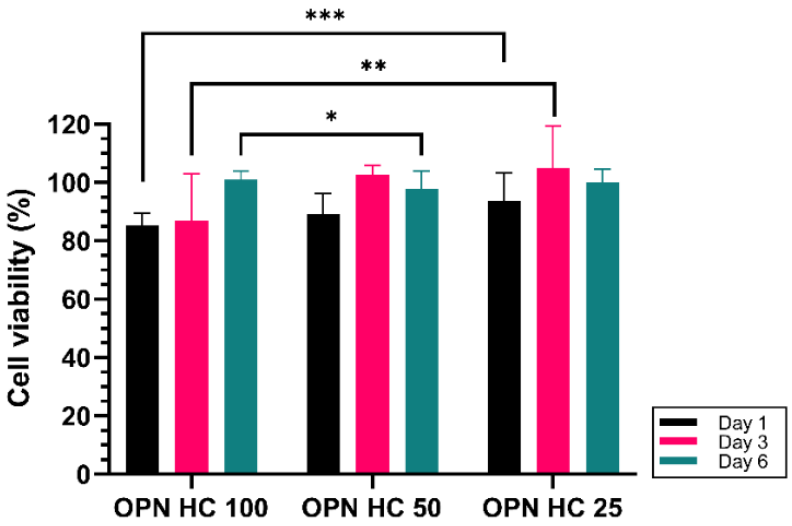


Figure 35 - Metabolic activity of MG63 cells after culture on Coll/nanoHA_Fb 1:2 HTb_OPN HC (100 µg/mL) sample with different elution's (only-substrate medium, 1:1 and 1:3, respectively) for 1, 3 and 6 days, estimated by Resazurin assay. the control, culture (TCPS) was considered 100% (*, significantly different comparing OPN HC 100 (only-substrate medium) with OPNC H 50 (1:1 substrate medium /cell culture medium) on the same time point (day 6), $p<0.028$); (**, significantly different comparing OPN HC 100 (only-substrate medium) with OPN HC 25 (1:3 substrate medium /cell culture medium) on the same time point (day 3), $p<0.028$); (***, significantly different comparing OPN HC 100 (only-substrate medium) with OPN HC 50 (1:1 substrate medium /cell culture medium) on the same time point (day 1), $p<0.015$).

To better understand the influence of OPN protein in cell viability and proliferation, figure 36 shows the cell viability of MG63 cells at day 6 of culture for all the samples without no elution (only composite medium). It could be observed that the OPN HC 100 indicates the highest cell viability (around 100%). Therefore, these results indicate an increase in cell proliferation rate with the OPN protein incorporation in the biocomposite. These results also indicated a lack of cytotoxicity of all the samples.

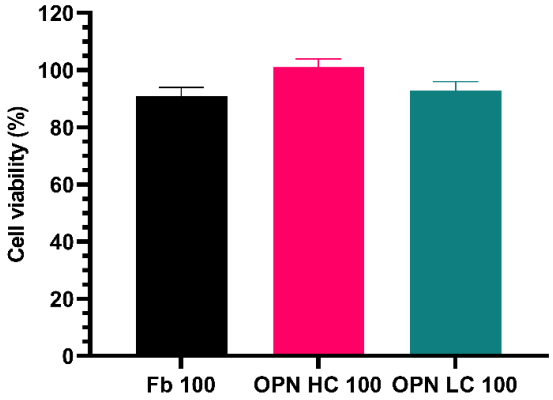


Figure 36 - Metabolic activity of MG63 cells after culture on Coll/nanoHA_Fb 1:2 HTb, Coll/nanoHA_Fb 1:2 HTb_OPN HC (100 µg/mL) and, Coll/nanoHA_Fb 1:2 HTb_OPN LC (10 µg/mL) sample for only-substrate medium for 6 days, estimated by Resazurin assay. the control, culture (TCPS) was considered 100%

4.3.2 Alkaline Phosphatase Activity

The functional activity of the cells on the Coll/nanoHA_Fb 1:2 HTb with and without the OPN protein was assessed by measuring the ALP activity after 6 days of culture. The results of ALP activity (Appendix A) showed an improved functional activity of MG63 cells with the biocomposite Coll/nanoHA_Fb 1:2 HTb. Moreover, no statistical differences were observed between the samples. The two-way ANOVA statistical test was performed for the different samples and no statistical difference was observed. Figure 37 shows the ALP activity for only-substrate medium to the different biocomposites. As it could be observed, Fb 100 was the sample with the highest expression of the osteoblastic phenotype. Nevertheless, the ALP activity showed a tendency to decrease with OPN lower concentration in the composite. Although, the highest concentration of OPN protein led to an increase in cell differentiation, the composite without OPN promoted a higher enzyme activity.

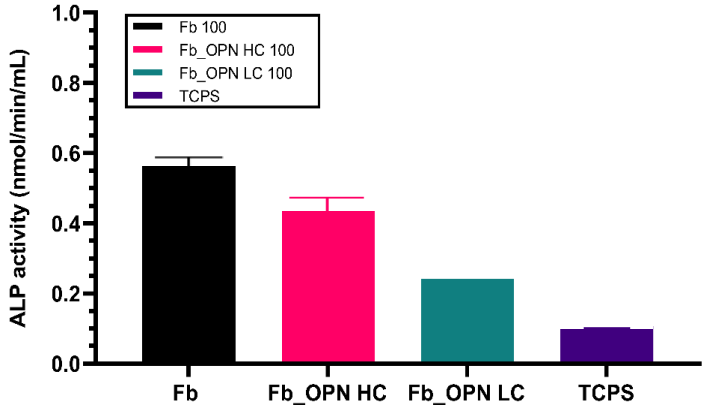


Figure 37 - ALP activity for osteoblastic phenotype expression of MG63 osteoblast-like cells culture for Coll/nanoHA_Fb 1:2 HTb, Coll/nanoHA_Fb 1:2 HTb_OPN HC (100 µg/mL), and Coll/nanoHA_Fb 1:2 HTb_ OPN LC (10 µg/mL) composite for only-substrate medium after culture at day 6.

4.3.3 Histocytochemical staining

The histocytochemical staining was carried out further to analyse the cellular osteogenic differentiation at 6 days of culture. All the results obtained are showed in Appendix B. The calcium phosphate deposition (Fig. 38) at day 6 of culture for the samples with only-substrate medium showed high mineral depositions to all the samples when compared to the TCPS sample (control). The highest concentration of calcium phosphate evidences the higher formation of the bone mineralization phase (red arrows). The highest ECM mineralization occurred in the OPN HC 100 sample, shown an improvement in mineral deposition with the incorporation of OPN protein.

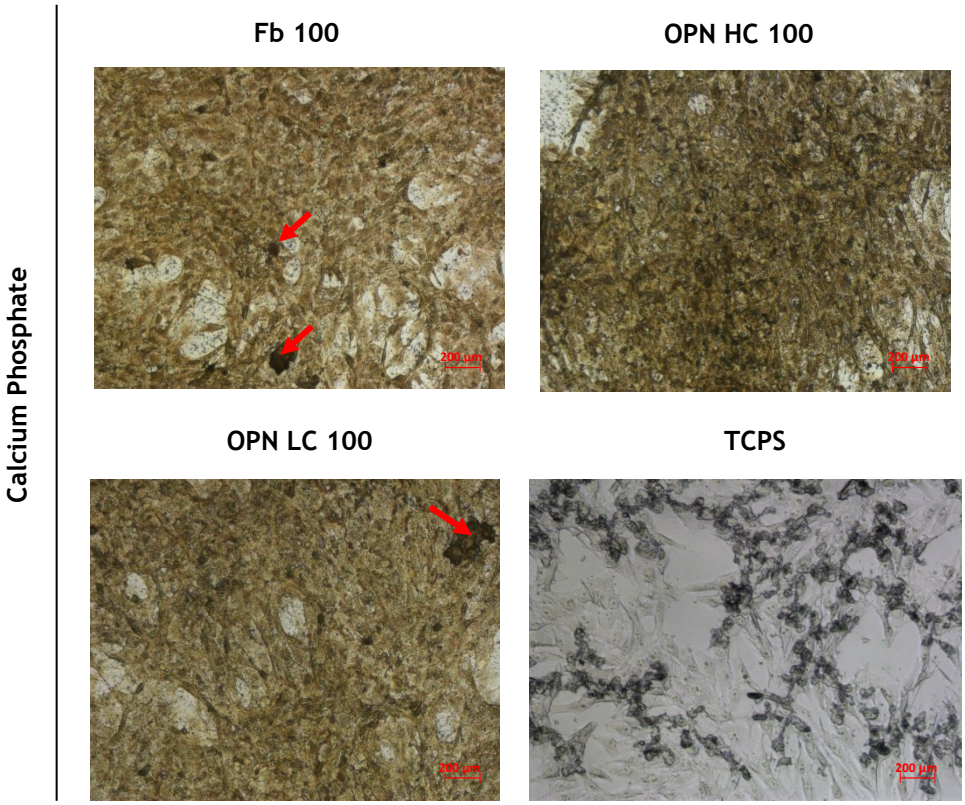


Figure 38 - Histomorphometric analysis for osteogenic differentiation of the MG63 cells after 6 days of culture with Fb 100, OPN HC 100, OPN LC 100 (eluate with degradation products), and TCPS samples. Von Kossa – Phosphate deposits stain. Scale: 200 µm. Red arrows evidence the ECM mineralization.

The type I collagen stanning (Sirius red) for all the samples is showed in Appendix B. Results showed higher collagen I deposition (osteogenic differentiation – similar to bone ECM) after 1, 3 and 6 days. Therefore, these results indicate an enhancement in protein deposition, which eventually will promote higher bone repair due to the biocomposite. Figure 39 shows the collagen I deposition on the Fb 100, OPN HC 100, OPN LC 100, and TCPS samples. Red arrows indicate collagen I, ECM deposition. These results evidence an improvement in collagen I presence between day 1, and day 6, which is enhanced by the osteogenic cell behaviour. It was possible to observe that the OPN protein promoted a higher production of collagen I.

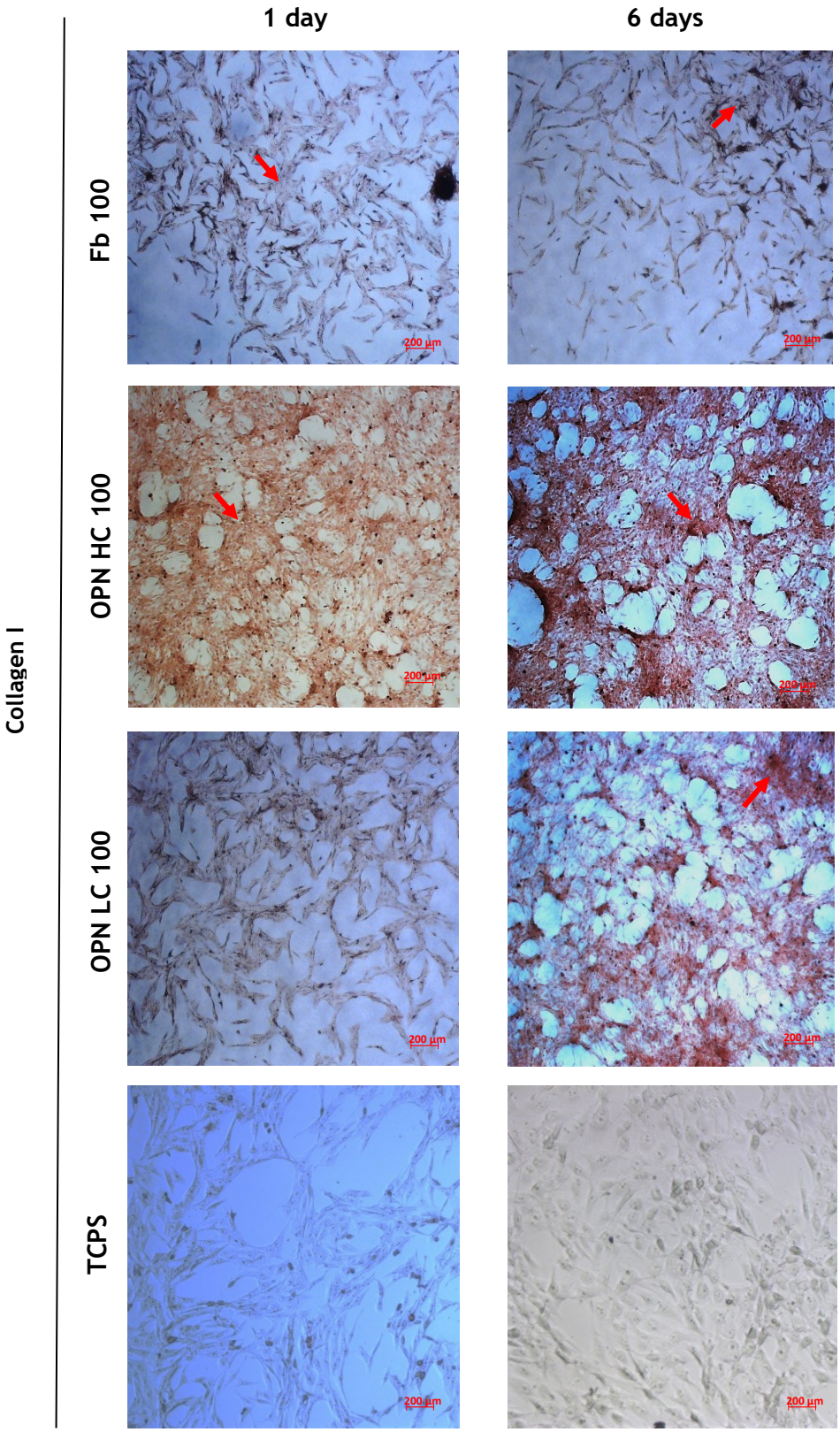


Figure 39 - Histomorphometric analysis for osteogenic differentiation of the MG63 cells after 6 days of culture with Fb 100, OPN HC 100, OPN LC 100 (eluate with degradation products), and TCPS samples. Sirius red for type I collagen stain. Scale: 200 µm. Red arrows evidence the higher protein deposition (cell ECM).

Chapter 5

Discussion

The main goal of this dissertation work was to develop a 3D Coll/nanoHA porous scaffold with fibrin hydrogel in order to improve the mechanical strength of the biomaterial and enhance bone tissue regeneration. The biomechanical/rheological properties of the composite (Coll/nanoHA scaffold + fibrin hydrogel with and without OPN) were tested by dynamic mechanical analysis (DMA) assay. DMA assay is a simple technique that is used to measuring the physical properties (e.g., Storage Modulus, Loss Modulus) by application of an oscillatory force to a sample and analysing the response of the material. The storage modulus (E') or elastic modulus describes the elastic mechanism of the material in storing energy to a predefined strain. The DMA results allow the measurement of the stiffness of the samples. Thus, the higher of E' modulus, the higher the stiffness of the material [43]. This technique is crucial for bone tissue engineering, allowing the simulation of the *in vivo* cyclic loading. Thus, this assay provides the study of the mechanical integrity of the scaffolds evaluating their biomechanical conditions to perform temporary mechanical support to the host site. The DMA results showed that the incorporation of fibrin hydrogels with Coll/nanoHA scaffolds resulted in an improvement in the final mechanical strength of the scaffold. Previous studies demonstrated that the incorporation of fibrin hydrogels within porous materials resulted in an improvement in the final strength of the composite (scaffold + fibrin gel). In the work by Brougham *et. al* [44], fibrin hydrogel was incorporated into the matrix of collagen and glycosaminoglycan (CG) scaffold, prepared by using a lyophilisation process. In this work was possible to analyse that the mechanical properties of the CG scaffold increased with the incorporation of fibrin hydrogel. The compressive modulus of fibrin hydrogel-only of 0.49 kPa ± 0.1, increased to 2.97 kPa ± 0.5 with the reinforcement of the CG scaffold. Another study by Foroushani *et.al* [45], showed that the incorporating of a gelatin-glycosaminoglycan (GG) electrospun matrix into a fibrin hydrogel provided an increase in the final mechanical properties. The Young's modulus and tensile strength of the fibrin gel with GG scaffold showed a significant increase of 0.662 ± 0.046 MPa and 0.886 ± 0.061 MPa, respectively.

However, the final biomechanical strength of the Coll/nanoHA scaffold is affected by varying the fibrinogen and thrombin concentrations in the final fibrin hydrogel. For hydrogels with a high concentration of thrombin, the grafts exhibited a higher mechanical strength. However, no statistical differences were observed. The results obtained showed that maintaining the thrombin concentration (1 NHI (U/mL)) but varying in fibrinogen concentration, the composite Coll/nanoHA_Fb 1:2 LTb with lower fibrinogen (6.3 mg/mL) showed a higher strength when compared to the composite Coll/nanoHA_Fb 1:1 LTb with higher fibrinogen concentration (10 mg/mL). In addition, maintaining the fibrinogen concentration (6.3 mg/mL) the composite Coll/nanoHA_Fb 1:2 LTb evidenced a lower mechanical strength when compared to the composite Coll/nanoHA_Fb 1:2 HTb, with higher thrombin concentration. In concordance with the literature review, fibrinogen is cleaved into fibrin due to the process initiated by the thrombin [36-39, 41]. Thus, the higher the concentrations of thrombin, the lower is the gelation time of the gel, which

results in a denser crosslinked structure, enhancing the final biomechanical properties of the gel and, subsequently, of the Coll/nanoHA scaffold. On the other hand, by reducing the thrombin concentration, the gel becomes more porous, leads a reduction in its final strength. Nevertheless, the spreading, proliferation, and differentiation of the cells are affected by the porosity of the matrix. Higher porosity of the hydrogel matrix promotes a decrease in the strength of the gel, decreasing the mechanical strength of the Coll/nanoHA scaffold. To improve the material's properties, the concentration of thrombin and fibrinogen was changed to achieve a better correlation between mechanical integrity and normal cell function [37]. The fibrin hydrogel Fb 1:2 HTb injected into Coll/nanoHA scaffold showed a higher mechanical resistance under compression solicitation. As result, the scaffold became stiffer, keeping their elastic behaviour. This composite showed a higher E' and E'' modulus when compared to the other composites materials. The tan δ results (Fig. 17) indicated that Coll/nanoHA scaffolds with fibrin hydrogel became more viscous and less elastic with the increase in frequency. Thus, the composite compression solicitations had a viscoelastic behaviour with a higher stiffness at a higher frequency when compared to lower ones, which leads to an appropriate behaviour for the regeneration of maxillofacial bone tissue.

The rheological properties of the composites with the OPN protein incorporation were tested for the composite Coll/nanoHA scaffold_Fb 1:2 HTb, which showed higher mechanical properties under compression without losing their ability to store energy, when compared to low thrombin samples. The rheometer analysis offers a rheological characterization of the material, studying the deformation and flow of the samples under an applied force. In this assay, an oscillatory shear stress force is applied to the samples displaying the mechanical characteristics of the materials (i.e., shear storage modulus (G') and shear loss modulus (G''')) [46]. The Coll/nanoHA_Fb 1:2 HTb with OPN at 10 µg/mL (LC) and 100 µg/mL (HC) showed a similar rheological characteristic, evidencing that the OPN protein does not negatively affect the mechanical response of the composite. In concordance with the literature review, the OPN protein is crucial in the modulation of osteoblasts, osteoclastic function, and matrix mineralization[12, 23, 46, 47]. Previous studies demonstrate that the OPN protein is crucial to promote the attachment of HA crystals, favouring the osteoblasts and osteoclast's adhesion, and subsequently promoting their growth and proliferation. Once this protein affects cellular function, the incorporation in fibrin hydrogel is a key aspect in mimicking ECM outside of the confined ECM. The normal OPN concentration in plasma blood is similar to the lower concentration (10 µg/mL) [22, 46, 47]. For the sample with lower OPN concentration the E' and E'' modulus showed very similar behaviour to the sample without the presence of the OPN, demonstrating that the OPN protein does not influence the rheological properties of the composite. Hence, with these mechanical results, the composite demonstrates a promissory mechanical behaviour to bone maxillofacial applications.

The rheological characteristics of the fibrin-only hydrogel were studied by rheometer analysis. The hydrogel samples showed mechanical behaviour in accordance with the DMA results. The Fb1:2 HTb was the hydrogel with the ideal rheological properties within the scaffold, presenting an improvement in the viscoelastic characteristics without losing their mechanical resistance. For bone tissue applications the material should be able to withstand stress applied, attain load-bearing properties, but also have the ability to store energy. Biologically, the tissues show nonlinear elastic behaviour to prevent large deformation [48]. Thus, the tissues become stiffer with an increasing of the strain. Fibrin hydrogels materials shown a viscoelastic behaviour, with both elastic and viscous characteristics. In agreement with the literature review, fibrinogen

and thrombin can be derived from the patient's own blood, and the final mechanics are directly linked to the concentrations of thrombin and fibrin [36-39, 41]. The fibrin structure is similar to the native tissue structure, which can induce in a short period of time the regeneration of damaged tissue. The mechanical properties of the fibrin gel are affected by the changes of stress applied to the matrix. As shown in figure 23 (G' modulus) and figure 25 (G'' modulus), the stiffness of the hydrogels increases with higher frequency applied. Since the cell behaviour within the construct is affected by the mechanical properties, higher hydrogel stability led to a higher cell proliferation rate and osteogenic differentiation. A higher concentration of fibrinogen and thrombin increases the gelation time, which directly affects the final structure of the gel matrix, decreasing their porosity and consequently the cell activity. Although, gelation time plays a key role in clinical application. The increase in polymerization rate is desired, however, the final architecture is denser, affecting the cell function within the construct. Thus, the modification in the fibrin properties becomes very important to achieve the optimal correlation between total porosity and polymerization time [36, 37, 39]. The rheometer results showed that fibrinogen at a constant concentration (6.3 mg/mL) and changing the thrombin solution (1 and 2 NHI (U/mL)), the hydrogel with lower thrombin concentration (Fb 1:2 LTb) presented a lower mechanical strength when compared to the hydrogel with higher thrombin concentration (Fb 1:2 HTb). Hence, these results elucidated that the increase in Tb concentration led to an increase in the mechanical strength of the gel. For the variation of fibrinogen concentration, but maintaining the Tb content, the hydrogels displayed a closer mechanical strength under shear stress forces (Fb 1:1 LTb and Fb 1:2 LTb). The increase of frequency led to an increase in G' and G'' for all the samples. This is the result of an increase in protein density as the fluid is expelled from the matrix of the gels during the shear compressive stress. Despite these mechanical differences, no statistical differences were observed. A previous work done by Chiu *et.al* [49], demonstrates that the Fb and Tb concentrations are directly linked to the permeability and stiffness of the 3D matrix of the fibrin gel. In this work, it was showed that the Fb and Tb dispute an inverse relationship, with the increase in Fb content to a Tb concentration of 2 or 5 IU/mL, the matrix permeability and average pore size decreased. Thus, the low concentration of Fb in the matrix structure of fibrin hydrogels supports greater diffusion and fluid. Directly linked with the porosity is the mechanical strength of the construct, decreasing with the increase of porosity. Another work by Rowe *et al.* [50], showed that the increase in thrombin concentrations led to an increase in the mechanical properties. The lower concentration of Tb resulted in a stiff 3D network structure, inversely higher concentrations forming dense ones.

In vitro biological studies were performed using human osteoblast-like cells (MG63) as a cell line. These cells are characterized by their high proliferation rate and their capability to easily differentiate into the osteogenic pathway *in vitro*. The cell viability assay is simple and accurate *in vitro* test that quantifies the number of live cells in a sample and monitors cell viability/ cytotoxicity. The higher the cellular metabolism, the higher the cell activity and, subsequently, the proliferation of the cells. Cell metabolic activity was assessed by the Alamar Blue assay (resazurin) which is a nontoxic technique. Hence, this assay allows the cytotoxicity evaluation of biomaterials when in contact with the cells. The cell viability and proliferation of the Coll/nanoHA_Fb 1:2 HTb with and without OPN, at high and low concentrations, were evaluated. The results showed that the material follows the safety concerns, showing high cell viability percentages (approximately >90% for all composites, with and without OPN protein). The elution medium with the degradation products of all samples (Fb 100, OPN HC 100, and OPN LC 100) showed similar cell viability when compared to the control with basic cell culture medium (TCPS)

after 1, 3, and 6 of cell culture. After the dilution (50% and 25%), it could be observed the same cellular metabolic activity for the same time-point (day 1). A previous work done by Parmar *et.al* [51], showed that cell viability in fibrin hydrogels scaffolds was above 100%, with a higher dependence on Fb content. For low Fb concentrations, the cell viability decreases with the time in culture due to low mechanical strength, which does not provide the optimal environment for cell growth and proliferate. At High Fb concentrations, the dense structure provides a compact environment for cells to proliferate and stay viable [51]. The cell viability in the composite with OPN protein incorporation showed a difference between the samples without OPN and with higher OPN concentrations. For lower OPN concentrations was possible to observe differences in the cell viability after 6 days. Nevertheless, it was expected that the number of cells and the metabolic activity would increase in the presence of this protein, since OPN favour cell adhesion. At the bone defect site, OPN protein plays a key role in further osteoblast differentiation. Subsequently, OPN provides high extracellular matrix deposition and mineralization [47].

Alkaline phosphatase activity (ALP) is an *in vitro* assay that quantifies the alkaline phosphatase enzyme. ALP is a common indicator of the expression of the osteoblastic phenotype. Thus, the ALP higher activity is associated with the cellular differentiation to bone cells phenotype and, subsequently the maturation of the extracellular matrix [50]. As it could be observed, the coll/nanoHA_Fb 1:2 HTb composite disputed a higher capacity in promoting new bone ECM formation with high levels of ALP activity at day 6. The presence of OPN protein showed higher cell differentiation at higher concentrations than at lower when compared with the control (basic medium). Previous studies done by Catelas *et.al* [42], showed that the Fibrin hydrogels with low Fb concentrations had a higher cell proliferation. However, high Fb concentrations showed an increase in ALP activity. Although, the Thrombin concentrations had a lesser effect. With this work was possible to observe that the proliferation and osteogenic differentiation in fibrin hydrogels is directly linked to the Fb/Tb ratio [42]. In bone repair process, thrombin plays a key role in the proliferation of osteoblasts. In addition, fibrin contributes for osteoblast differentiation and bone healing. Fibrinogen favour a higher environment for cell proliferation and differentiation due to high fibronectin binding capacity. Fibronectin regulates the adhesion, proliferation, and differentiation of osteoblasts [49, 52].

Histocytochemical staining analysis was performed to evaluate the material's osteogenic induction. The red colour of the cells represented the collagen type I deposition (cellular ECM) produced by the differentiated osteoblasts. Results showed that with the time in culture, the Coll content in the ECM increased. It could also be observed the mineral deposits in the MG63 cells extracellular matrix (calcium phosphates are the brownish rounded shape) by histocytochemical staining for phosphate (Von Kossa) (Fig.37). All the composites degradation products incubation, when compared to the control with only basic cell culture medium, showed an increase of calcium phosphate deposition at day 6 of culture. Hence, based on the *in vitro* response of the composite, it was possible to observe an optimal tendency in osteogenic differentiation induction without any cytotoxicity response. Previous works done by Salgado *et.al* [53], showed that cryogels Coll/nanoHA scaffolds are able to differentiate HBMSCs cells into osteoblastic phenotype. Another work done by Rodrigues *et.al* [54], showed that the Coll/nanoHA biocomposite had higher cell proliferation when compared to the only-Collagen scaffold. Previous works evidence an optimal osteoblast proliferation rate, and osteogenic differentiation in fibrin hydrogels scaffolds [42, 48-50, 55]. Therefore, the combination of Fibrin hydrogels with Coll/nanoHA scaffold result in a potential solution to successfully promote bone cell proliferation and differentiation, increasing the bone tissue growth within the bone defect site.

Chapter 6

Conclusion and Future Outlook

Bone maxillofacial regeneration challenges are associated with multi factors: the difficulty to achieve extracellular biomimetic requirements, the inability to produce complex, but more functional cellular structures in large 3D scaffolds, and the lack of strategies to induce vasculature regeneration. This project developed a Coll/nanoHA/Fb scaffold in order to offer an innovative solution to treat maxillofacial bone defects. The incorporation of fibrin a modified hydrogel with a Coll/nanoHA scaffold biomaterial showed an improvement in the final mechanical strength of the graft. Fibrin gel is a versatile biomaterial extensity applied for bone tissue repair due to network structure, mechanical properties, and stability. This current characteristic could be designed and controlled by the polymerization process. The fibrin and thrombin concentration plays a key role in the final mechanics and biological characteristics. Therefore, fibrin-cell interactions are directly affected. With this work, it was possible to observe that the strength of the fibrin hydrogel increased with the Tb content. Subsequently, the mechanical properties of the scaffold were enhanced. Rheological analysis showed a non-linear behaviour of the fibrin hydrogel, presenting viscoelastic properties under dynamic compression. Hence, increasing the shear stress forces applied to the matrix of the hydrogel led to a polymeric chain network reorganization the increasing the polymer density promoting an increase of materials' stiffness [36]. This hardening behaviour showed an excellent capacity to withstand load-bearing applications. Mechanically, the OPN incorporation within the 3D composite scaffold did not negatively affect the strength of the composite. For a Fb hydrogel content of 6.3 mg/mL of fibrinogen and 2 NHI (U/mL) of thrombin, the Coll/nanoHA scaffold improved the final mechanical strength, maintaining its elasticity. For an optimal Fb/Tb content, the composite was biologically analysed, showing high biocompatibility, increasing the new bone-cell differentiation with time culture. On day 6 of cell culture, the cells cultured with composite's degradation products showed higher new bone extracellular matrix deposition. The OPN protein promoted an increase in osteogenic cell differentiation. Hence, this composite in the presence of OPN protein showed higher biocompatibility and cellular differentiation, with a higher capacity in promoting new bone ECM formation.

Coll/nanoHA/Fb biocomposite was shown as a potential solution to improve successful regeneration in patients with critical maxillofacial bone defects, offers an innovative 3D scaffold solution to boost fully bone tissue regeneration and early recovery of the patients. Nevertheless, more studies are needed to achieve the optimal relationship between mechanical properties and the polymerization process of the OPN-modified fibrin hydrogel.

References

[1] R. F. Canadas, S. Pina, A. P. Marques, J. M. Oliveira, and R. L. Reis, "Chapter 7 - Cartilage and Bone Regeneration—How Close Are We to Bedside?," in *Translating Regenerative Medicine to the Clinic*, J. Laurence, Ed. Boston: Academic Press, 2016, pp. 89-106.

[2] A. R. Amini, C. T. Laurencin, and S. P. Nukavarapu, "Bone tissue engineering: recent advances and challenges," (in eng), *Critical reviews in biomedical engineering,* vol. 40, no. 5, pp. 363-408, 2012.

[3] A. Oryan, S. Alidadi, A. Moshiri, and N. Maffulli, "Bone regenerative medicine: classic options, novel strategies, and future directions," (in eng), *Journal of orthopaedic surgery and research,* vol. 9, no. 1, pp. 18-18, 2014.

[4] F. Akter and J. Ibanez, "Chapter 8 - Bone and Cartilage Tissue Engineering," in *Tissue Engineering Made Easy*, F. Akter, Ed.: Academic Press, 2016, pp. 77-97.

[5] R. Dimitriou, E. Jones, D. McGonagle, and P. V. Giannoudis, "Bone regeneration: current concepts and future directions," *BMC Medicine,* vol. 9, no. 1, p. 66, 2011/05/31 2011.

[6] X. Bai, M. Gao, S. Syed, J. Zhuang, X. Xu, and X.-Q. Zhang, "Bioactive hydrogels for bone regeneration," *Bioactive Materials,* vol. 3, pp. 401-417, 05/26 2018.

[7] M. Ansari, "Bone tissue regeneration: biology, strategies and interface studies," *Progress in Biomaterials,* vol. 8, no. 4, pp. 223-237, 2019/12/01 2019.

[8] M. Meskinfam, "17 - Polymer scaffolds for bone regeneration," in *Characterization of Polymeric Biomaterials*, M. C. Tanzi and S. Farè, Eds.: Woodhead Publishing, 2017, pp. 441-475.

[9] A. M. Grumezescu, "6.5.4 Nanocomposites Based on HA and Collagen," in *Nanobiomaterials in Hard Tissue Engineering - Applications of Nanobiomaterials*: Elsevier.

[10] R. C. Riddle and T. L. Clemens, "Bone Cell Bioenergetics and Skeletal Energy Homeostasis," *Physiological Reviews,* vol. 97, no. 2, pp. 667-698, 2017.

[11] A. M. Mohamed, "An overview of bone cells and their regulating factors of differentiation," (in eng), *The Malaysian journal of medical sciences : MJMS,* vol. 15, no. 1, pp. 4-12, 2008.

[12] T. Bellido, L. I. Plotkin, and A. Bruzzaniti, "Chapter 3 - Bone Cells," in *Basic and Applied Bone Biology (Second Edition)*, D. B. Burr and M. R. Allen, Eds.: Academic Press, 2019, pp. 37-55.

[13] P. Garnero, "The Role of Collagen Organization on the Properties of Bone," *Calcified Tissue International,* vol. 97, no. 3, pp. 229-240, 2015/09/01 2015.

[14] S. Viguet-Carrin, P. Garnero, and P. Delmas, "The role of collagen in bone strength," *Osteoporosis international : a journal established as result of cooperation between the European Foundation for Osteoporosis and the National Osteoporosis Foundation of the USA,* vol. 17, pp. 319-36, 02/01 2006.

[15] X. Zhang, "12.4 Mechanical Properties," in *Science and Principles of Biodegradable and Bioresorbable Medical Polymers - Materials and Properties*: Elsevier.

[16] B. Lowe, J. G. Hardy, and L. J. Walsh, "Optimizing Nanohydroxyapatite Nanocomposites for Bone Tissue Engineering," (in eng), *ACS omega,* vol. 5, no. 1, pp. 1-9, 2019.

[17] G. Molino, M. C. Palmieri, G. Montalbano, S. Fiorilli, and C. Vitale-Brovarone, "Biomimetic and mesoporous nano-hydroxyapatite for bone tissue application: a short review," *Biomedical Materials,* vol. 15, no. 2, p. 022001, 2020/02/27 2020.

[18] A. M. Grumezescu, "6.1 Introduction," in *Nanobiomaterials in Hard Tissue Engineering - Applications of Nanobiomaterials*: Elsevier.

[19] M. S. Ghiasi, J. Chen, A. Vaziri, E. K. Rodriguez, and A. Nazarian, "Bone fracture healing in mechanobiological modeling: A review of principles and methods," (in eng), *Bone reports,* vol. 6, pp. 87-100, 2017.

[20] A. Schindeler, M. M. McDonald, P. Bokko, and D. G. Little, "Bone remodeling during fracture repair: The cellular picture," *Seminars in Cell & Developmental Biology,* vol. 19, no. 5, pp. 459-466, 2008/10/01/ 2008.

[21] M. A. Icer and M. Gezmen-Karadag, "The multiple functions and mechanisms of osteopontin," *Clinical Biochemistry,* vol. 59, pp. 17-24, 2018/09/01/ 2018.

[22] A. Singh, G. Gill, H. Kaur, M. Amhmed, and H. Jakhu, "Role of osteopontin in bone remodeling and orthodontic tooth movement: a review," *Progress in Orthodontics,* vol. 19, no. 1, p. 18, 2018/06/25 2018.

[23] P. J. Thurner *et al.*, "Osteopontin deficiency increases bone fragility but preserves bone mass," *Bone,* vol. 46, no. 6, pp. 1564-1573, 2010/06/01/ 2010.

[24] H. Qu, H. Fu, Z. Han, and Y. Sun, "Biomaterials for bone tissue engineering scaffolds: a review," *RSC Advances,* 10.1039/C9RA05214C vol. 9, no. 45, pp. 26252-26262, 2019.

[25] F. J. O'Brien, "Biomaterials & scaffolds for tissue engineering," *Materials Today,* vol. 14, no. 3, pp. 88-95, 2011/03/01/ 2011.

[26] P. Kubasiewicz-Ross *et al.*, "New nano-hydroxyapatite in bone defect regeneration: A histological study in rats," *Annals of Anatomy - Anatomischer Anzeiger,* vol. 213, pp. 83-90, 2017/09/01/ 2017.

[27] X. C. Ing Zhu. (2012). *Biofabrication of Tissue Scaffolds: Advances in Biomaterials Science and Biomedical Applications.*

[28] F. Wahid, T. Khan, Z. Hussain, and H. Ullah, "30 - Nanocomposite scaffolds for tissue engineering; properties, preparation and applications," in *Applications of Nanocomposite Materials in Drug Delivery*, Inamuddin, A. M. Asiri, and A. Mohammad, Eds.: Woodhead Publishing, 2018, pp. 701-735.

[29] S. C. Rodrigues, C. L. Salgado, A. Sahu, M. P. Garcia, M. H. Fernandes, and F. J. Monteiro, "Preparation and characterization of collagen-nanohydroxyapatite biocomposite scaffolds by cryogelation method for bone tissue engineering applications," *Journal of Biomedical Materials Research Part A,* vol. 101A, no. 4, pp. 1080-1094, 2013.

[30] F. Ullah, M. B. H. Othman, F. Javed, Z. Ahmad, and H. M. Akil, "Classification, processing and application of hydrogels: A review," *Materials Science and Engineering: C,* vol. 57, pp. 414-433, 2015/12/01/ 2015.

[31] M. B. Sordi, A. Cruz, M. C. Fredel, R. Magini, and P. T. Sharpe, "Three-dimensional bioactive hydrogel-based scaffolds for bone regeneration in implant dentistry," *Materials Science and Engineering: C,* vol. 124, p. 112055, 2021/05/01/ 2021.

[32] M. Liu *et al.*, "Injectable hydrogels for cartilage and bone tissue engineering," *Bone Research,* vol. 5, 05/30 2017.

[33] S. Yue, H. He, B. Li, and T. Hou, "Hydrogel as a Biomaterial for Bone Tissue Engineering: A Review," (in eng), *Nanomaterials (Basel, Switzerland),* vol. 10, no. 8, p. 1511, 2020.

[34] W. Zhao, X. Jin, Y. Cong, Y. Liu, and J. Fu, "Degradable natural polymer hydrogels for articular cartilage tissue engineering," *Journal of Chemical Technology & Biotechnology,* vol. 88, no. 3, pp. 327-339, 2013.

[35] Y. Sun, D. Nan, H. Jin, and X. Qu, "Recent advances of injectable hydrogels for drug delivery and tissue engineering applications," *Polymer Testing,* vol. 81, p. 106283, 2020/01/01/ 2020.

[36] A. Noori, S. J. Ashrafi, R. Vaez-Ghaemi, A. Hatamian-Zaremi, and T. J. Webster, "A review of fibrin and fibrin composites for bone tissue engineering," (in eng), *International journal of nanomedicine,* vol. 12, pp. 4937-4961, 2017.

[37] E. Sproul, S. Nandi, and A. Brown, "6 - Fibrin biomaterials for tissue regeneration and repair," in *Peptides and Proteins as Biomaterials for Tissue Regeneration and Repair*, M. A. Barbosa and M. C. L. Martins, Eds.: Woodhead Publishing, 2018, pp. 151-173.

[38] P. A. Janmey, J. P. Winer, and J. W. Weisel, "Fibrin gels and their clinical and bioengineering applications," *Journal of the Royal Society Interface,* vol. 6, no. 30, pp. 1-10, 2009.

[39] J. W. Weisel and R. I. Litvinov, "Fibrin Formation, Structure and Properties," (in eng), *Sub-cellular biochemistry,* vol. 82, pp. 405-456, 2017.

[40] J.-H. Oh, H.-J. Kim, T.-I. Kim, J.-H. Baek, H.-M. Ryoo, and K. M. Woo, "The effects of the modulation of the fibronectin-binding capacity of fibrin by thrombin on osteoblast differentiation," *Biomaterials,* vol. 33, no. 16, pp. 4089-4099, 2012/06/01/ 2012.

[41] B.-S. Kim, H.-M. Sung, H.-K. You, and J. Lee, "Effects of fibrinogen concentration on fibrin glue and bone powder scaffolds in bone regeneration," *Journal of Bioscience and Bioengineering,* vol. 118, no. 4, pp. 469-475, 2014/10/01/ 2014.

[42] "Human Mesenchymal Stem Cell Proliferation and Osteogenic Differentiation in Fibrin Gels in Vitro," *Tissue Engineering,* vol. 12, no. 8, pp. 2385-2396, 2006.

[43] K. P. Menard, *DYNAMIC MECHANICAL ANALYSIS - A Pratical Introduction*, 2º edition ed. Taylor & Francis Group, LLC

CRC Press is an imprint of Taylor & Francis, 2008.

[44] C. M. Brougham, T. J. Levingstone, S. Jockenhoevel, T. C. Flanagan, and F. J. O'Brien, "Incorporation of fibrin into a collagen–glycosaminoglycan matrix results in a scaffold with improved mechanical properties and enhanced capacity to resist cell-mediated contraction," *Acta Biomaterialia,* vol. 26, pp. 205-214, 2015/10/15/ 2015.

[45] Z. H. Foroushani, S. S. Mahdavi, M. J. Abdekhodaie, A. Baradaran-Rafii, M. r. Tabatabei, and M. Mehrvar, "A hybrid scaffold of gelatin glycosaminoglycan matrix and fibrin as a carrier of human corneal fibroblast cells," *Materials Science and Engineering: C,* vol. 118, p. 111430, 2021/01/01/ 2021.

[46] M. Gordjestani, L. Dermaut, L. De Ridder, and P. De Waele, "Osteopontin and bone repair in rabbit tibial defect," *European Journal of Orthopaedic Surgery & Traumatology,* vol. 17, no. 2, pp. 139-145, 2007/03/01 2007.

[47] M. D. McKee, C. E. Pedraza, and M. T. Kaartinen, "Osteopontin and wound healing in bone," (in eng), *Cells Tissues Organs,* vol. 194, no. 2-4, pp. 313-9, 2011.

[48] M. A. Al Enezy-Ulbrich *et al.*, "Impact of Reactive Amphiphilic Copolymers on Mechanical Properties and Cell Responses of Fibrin-Based Hydrogels," *Advanced Functional Materials,* vol. 30, no. 38, p. 2003528, 2020.

[49] C. Chiu, V. Hecht, H. Duong, B. Wu, and B. Tawil, "Permeability of Three-Dimensional Fibrin Constructs Corresponds to Fibrinogen and Thrombin Concentrations," *BioResearch open access,* vol. 1, pp. 34-40, 02/01 2012.

[50] S. L. Rowe, S. Lee, and J. P. Stegemann, "Influence of thrombin concentration on the mechanical and morphological properties of cell-seeded fibrin hydrogels," *Acta Biomaterialia,* vol. 3, no. 1, pp. 59-67, 2007/01/01/ 2007.

[51] A. Parmar, N. A. Ansari, G. Parmar, and A. Krishnakumar, "Evaluation of cell viability of Human Dental Pulp Stem Cells in Two dimensional and Three dimensional Fibrin Glue Scaffold," (in eng), *Journal of conservative dentistry : JCD,* vol. 23, no. 5, pp. 479-483, Sep-Oct 2020.

[52] J.-H. Oh, H.-J. Kim, T.-I. Kim, and K. M. Woo, "Comparative evaluation of the biological properties of fibrin for bone regeneration," (in eng), *BMB reports,* vol. 47, no. 2, pp. 110-114, 2014.

[53] C. L. Salgado, L. Grenho, M. H. Fernandes, B. J. Colaço, and F. J. Monteiro, "Biodegradation, biocompatibility, and osteoconduction evaluation of collagen-nanohydroxyapatite cryogels for bone tissue regeneration," (in eng), *J Biomed Mater Res A,* vol. 104, no. 1, pp. 57-70, Jan 2016.

[54] S. C. Rodrigues, C. L. Salgado, A. Sahu, M. P. Garcia, M. H. Fernandes, and F. J. Monteiro, "Preparation and characterization of collagen-nanohydroxyapatite biocomposite scaffolds by cryogelation method for bone tissue engineering applications," (in eng), *J Biomed Mater Res A,* vol. 101, no. 4, pp. 1080-94, Apr 2013.

[55] J.-I. Sasaki, T. Matsumoto, and S. Imazato, "Oriented bone formation using biomimetic fibrin hydrogels with three-dimensional patterned bone matrices," *Journal of Biomedical Materials Research Part A,* vol. 103, no. 2, pp. 622-627, 2015.

Appendix A – ALP activity for osteoblastic phenotype expression of MG63 osteoblast-like cells

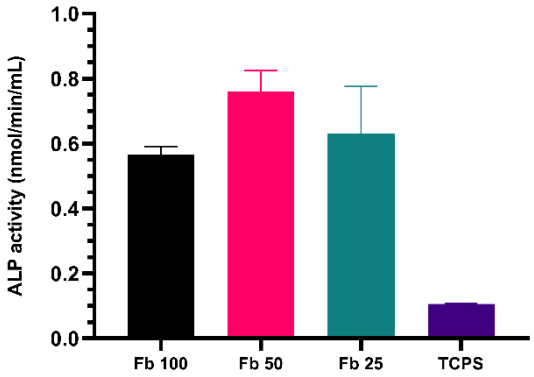


Figure 40 - ALP activity for osteoblastic phenotype expression of MG63 osteoblast-like cells culture for Coll/nanoHA scaffold_Fb 1:2 HTb composite with different concentration substrate medium/ cell culture medium (only-composite, 1:1 and 1:3) after culture at day 6.

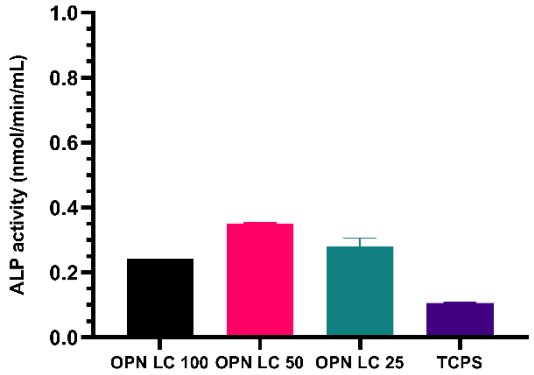


Figure 41 - ALP activity for osteoblastic phenotype expression of MG63 osteoblast-like cells culture for Coll/nanoHA_Fb 1:2 HTb_OPN LC (10 µg/mL) composite with different concentration substrate medium/ cell culture medium (only-composite, 1:1 and 1:3) after culture at day 6.

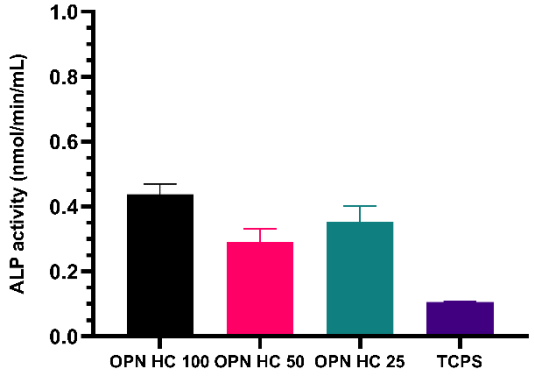


Figure 42 - ALP activity for osteoblastic phenotype expression of MG63 osteoblast-like cells culture for Coll/nanoHA_Fb 1:2 HTb_OPN HC (100 µg/mL) composite with different concentration substrate medium/ cell culture medium (only-composite, 1:1 and 1:3) after culture at day 6.

Appendix B - Optical *In Vitro* of histocytochemical staining for osteoblastic phenotype expression of MG63 osteoblast-like cells

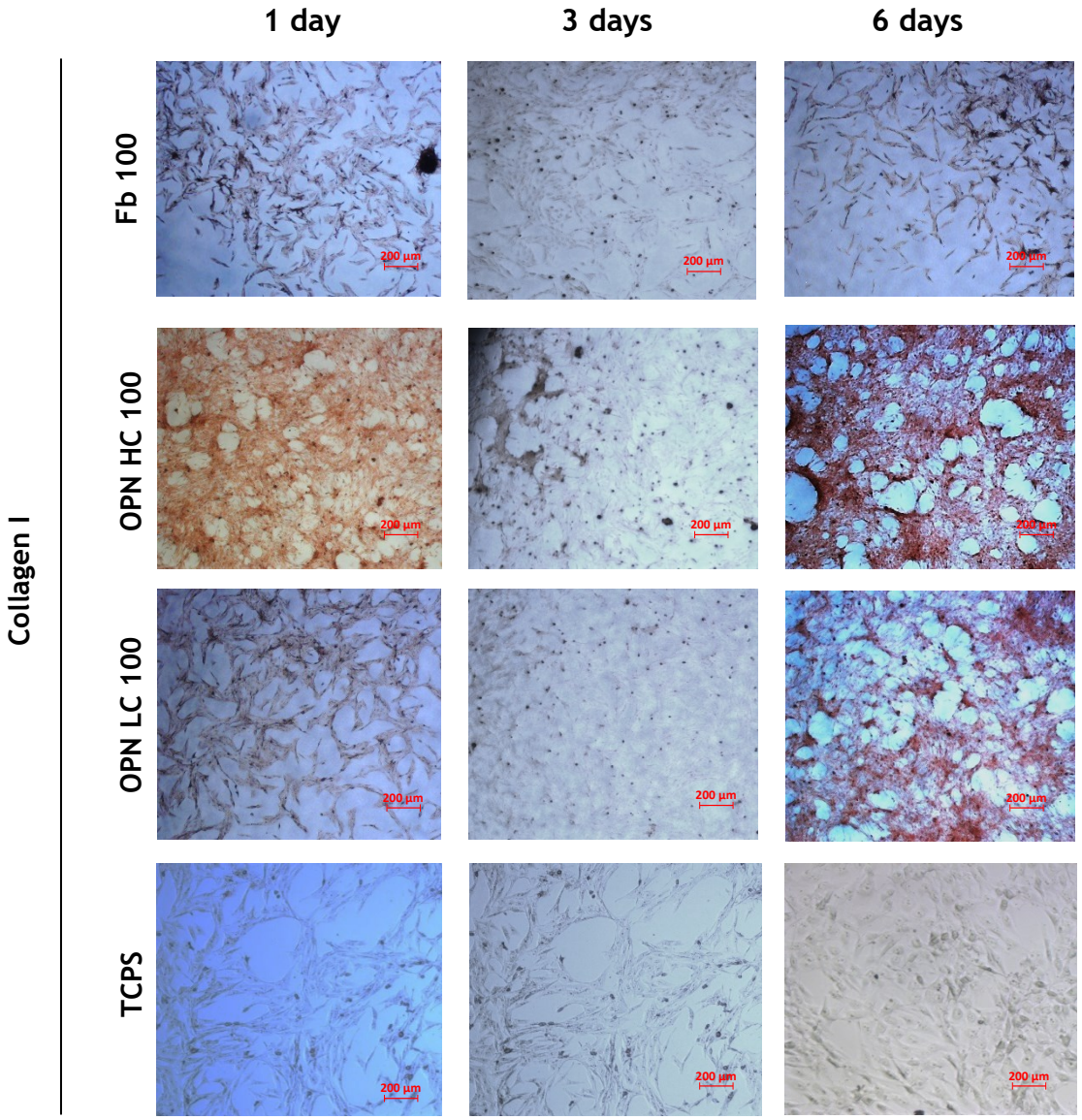


Figure 43 - Histomorphometric analysis for osteogenic differentiation of the MG63 cells after 1, 3 and 6 days of culture with Fb 100, OPN HC 100, OPN LC 100 (eluate with degradation products), and TCPS samples. Sirius red for type I collagen stain. Scale: 200 µm.

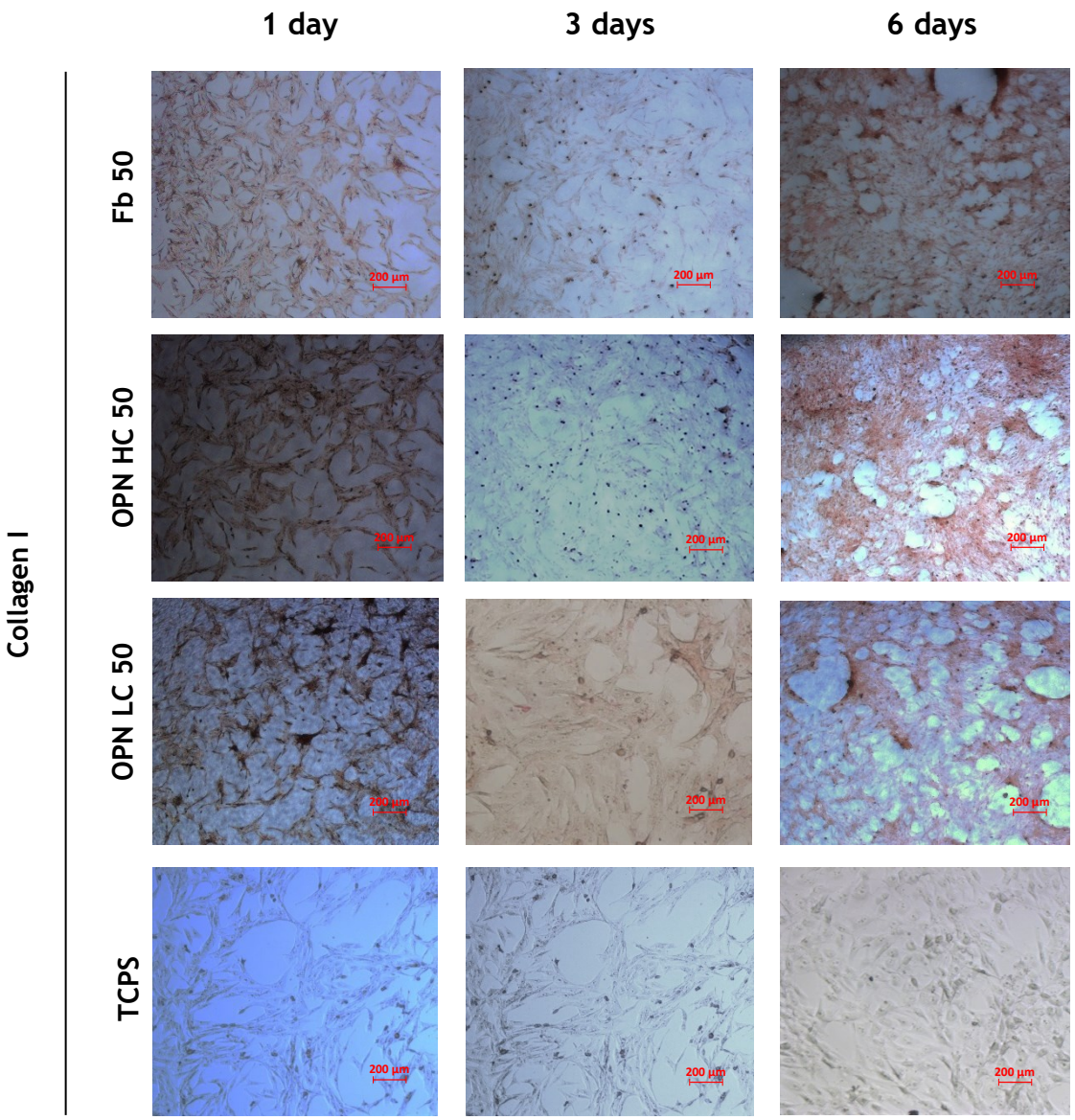


Figure 44 - Histomorphometric analysis for osteogenic differentiation of the MG63 cells after 1, 3 and 6 days of culture with Fb 50, OPN HC 50, OPN LC 50 (eluate with degradation products), and TCPS samples. Sirius red for type I collagen stain. Scale: 200 µm.

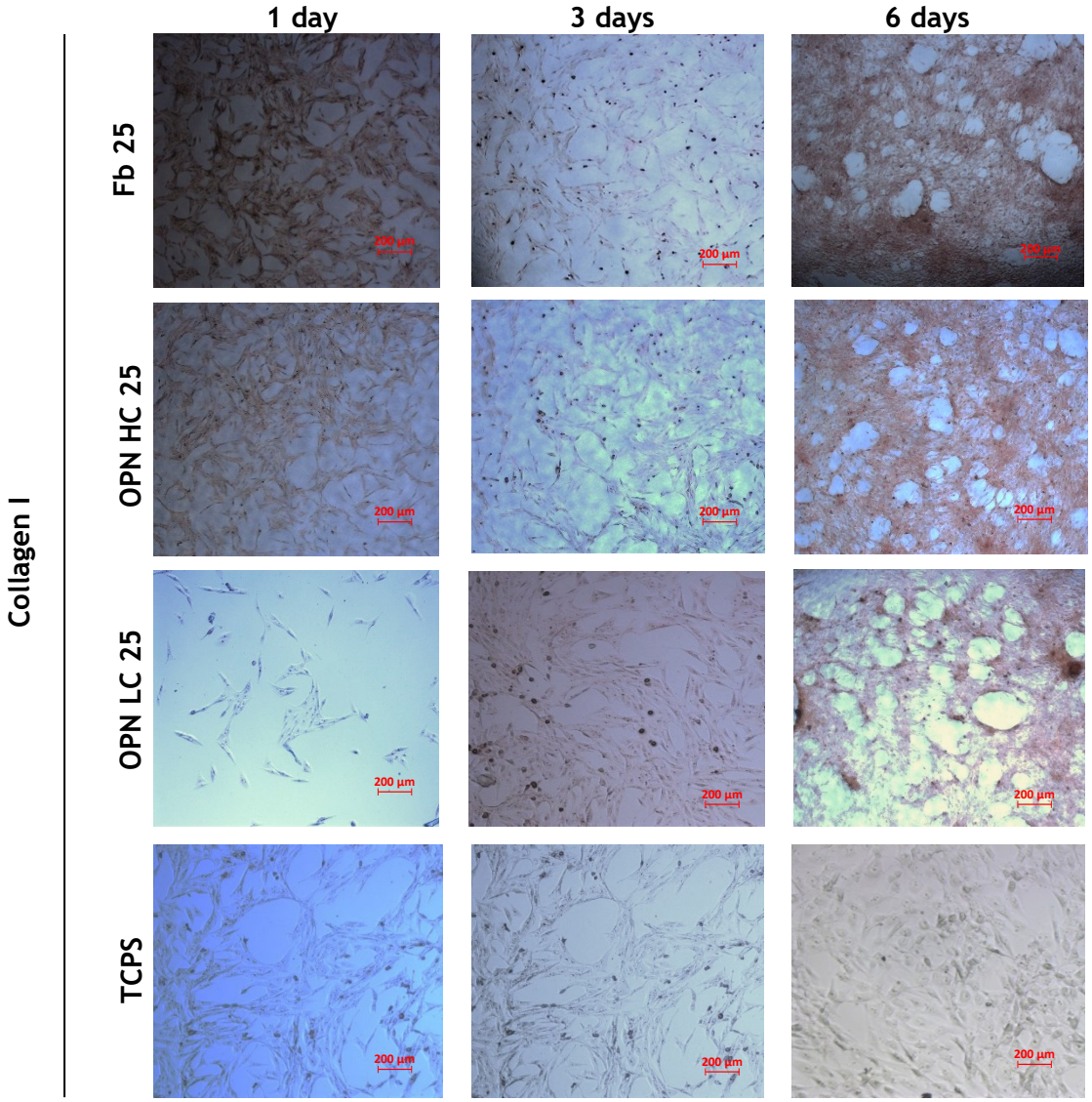


Figure 45 - Histomorphometric analysis for osteogenic differentiation of the MG63 cells after 1, 3 and 6 days of culture with Fb 25, OPN HC 25, OPN LC 25 (eluate with degradation products), and TCPS samples. Sirius red for type I collagen stain. Scale: 200 µm.

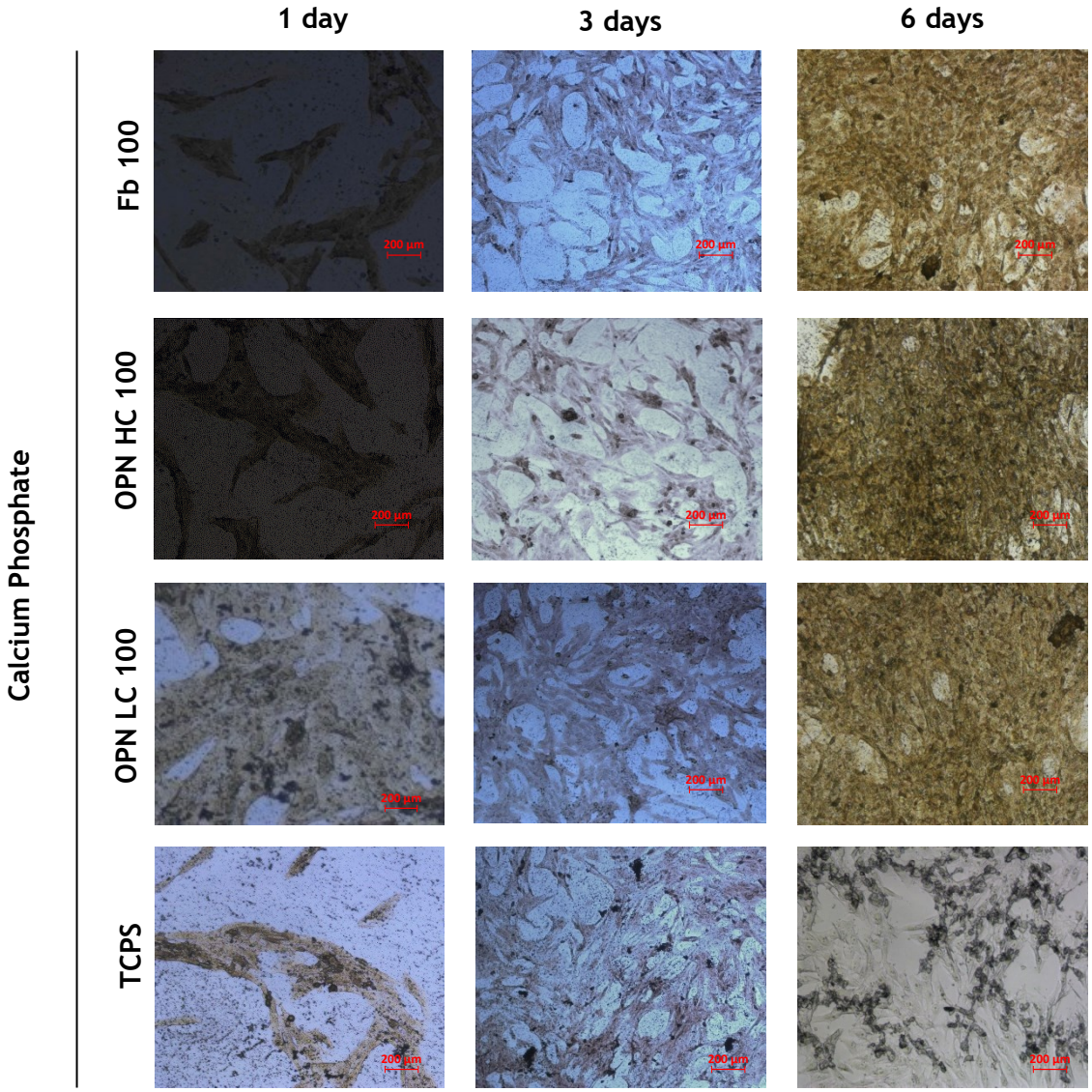


Figure 46 - Histomorphometric analysis for osteogenic differentiation of the MG63 cells after 1, 3 and 6 days of culture with Fb 100, OPN HC 100, OPN LC 100 (eluate with degradation products), and TCPS samples. Von Kossa – Phosphate deposits stain. Scale: 200 µm

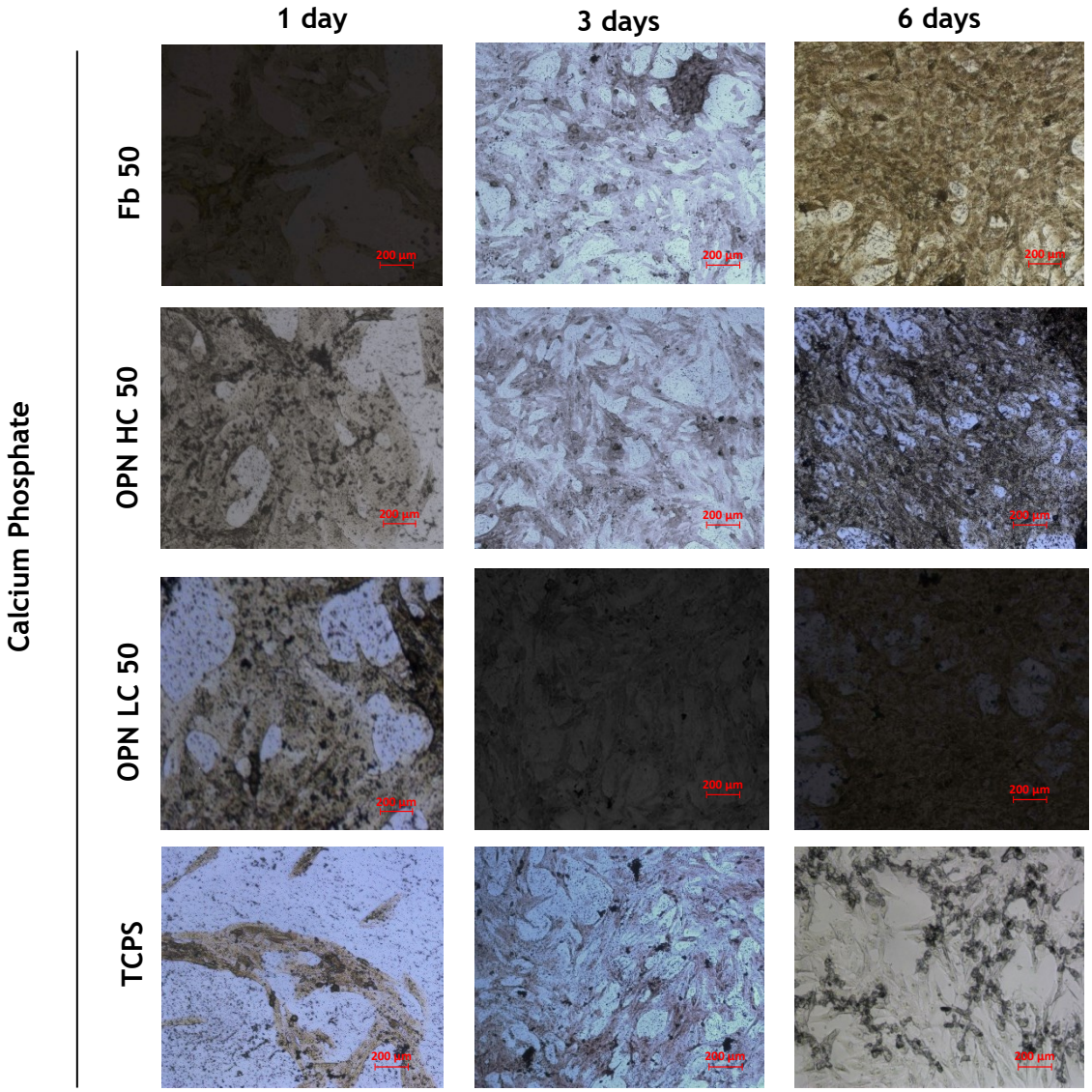


Figure 47 - Histomorphometric analysis for osteogenic differentiation of the MG63 cells after 1, 3 and 6 days of culture with Fb 50, OPN HC 50, OPN LC 50 (eluate with degradation products), and TCPS samples. Von Kossa – Phosphate deposits stain. Scale: 200 µm

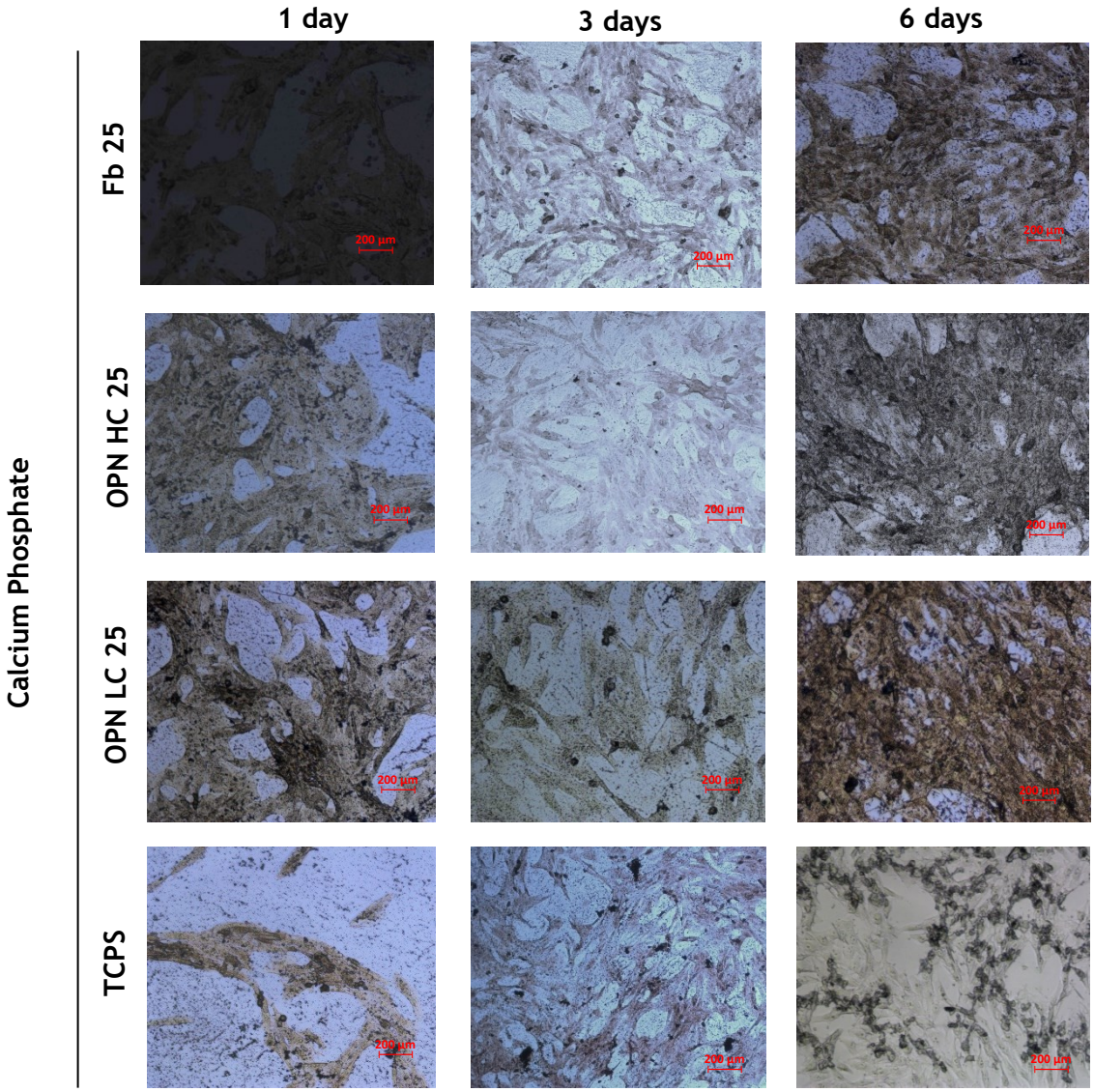


Figure 48 - Histomorphometric analysis for osteogenic differentiation of the MG63 cells after 1, 3 and 6 days of culture with Fb 25, OPN HC 25, OPN LC 25 (eluate with degradation products), and TCPS samples. Von Kossa – Phosphate deposits stain. Scale: 200 µm